EUROPEAN CENTRAL BANK

WORKING PAPER SERIES

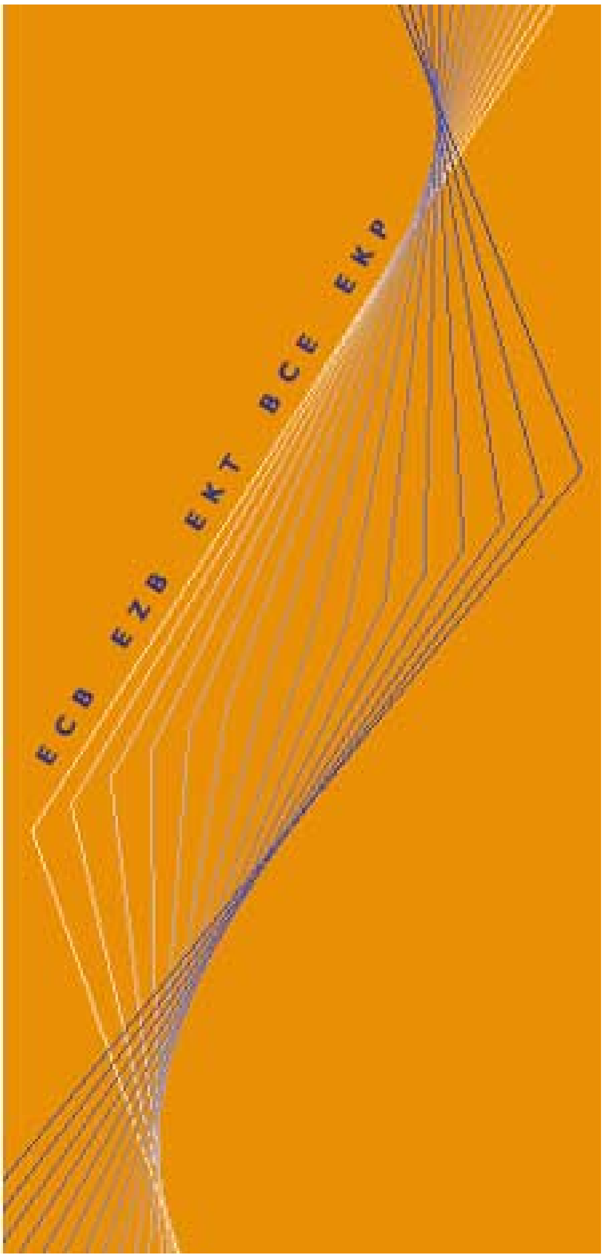

WORKING PAPER NO. 23

ESCAPING NASH INFLATION

BY IN-KOO CHO AND
THOMAS J. SARGENT

JUNE 2000

EUROPEAN CENTRAL BANK

WORKING PAPER SERIES

WORKING PAPER NO. 23

ESCAPING NASH INFLATION

BY IN-KOO CHO AND
THOMAS J. SARGENT*

JUNE 2000

* *We thank George Evans, Lars Peter Hansen, Michael Harrison, Seppo Honkapohja, Kenneth Judd, Robert King and David M. Kreps for helpful discussions. Chao Wei helped with the simulations. Financial support from the National Science Foundation is gratefully acknowledged.*
In-Koo Cho, University of Illinois, Urbana-Champaign and Thomas J. Sargent, Stanford University and Hoover Institution.

Address	**Kaiserstrasse 29**
	D-60311 Frankfurt am Main
	Germany
Postal address	**Postfach 16 03 19**
	D-60066 Frankfurt am Main
	Germany
Telephone	**+49 69 1344 0**
Internet	**http://www.ecb.int**
Fax	**+49 69 1344 6000**
Telex	**411 144 ecb d**

ISSN 1561-0810

Contents

Abstract

Mean dynamics govern convergence to rational expectations equilibria of self-referential systems under least squares learning. We highlight *escape dynamics* that propel away from a rational expectations equilibrium under fixed-gain recursive learning schemes. These learning schemes discount past observations. In a model with a unique self-confirming equilibrium, we show that the destination of the escape dynamics is an outcome associated with government discovery of too strong a version of the natural rate hypothesis. That destination is not sustainable as a self-confirming equilibrium but is visited recurrently. The escape route dynamics cause recurrent outcomes close to the Ramsey (commitment) inflation rate in a model with an adaptive government.

Key Words: Self-confirming equilibrium, mean dynamics, escape route, large deviation, natural rate of unemployment, adaptation, experimentation trap.

'If an unlikely event occurs, it is very likely to occur in the most likely way.'

Michael Harrison

1 Introduction

Building on work by Sims (1988) and Chung (1990), Sargent (1999) studied a setting in which adaptation within an approximating Phillips curve model causes recurrent escapes from the time-consistent outcome of Kydland and Prescott (1977). Better outcomes emerge

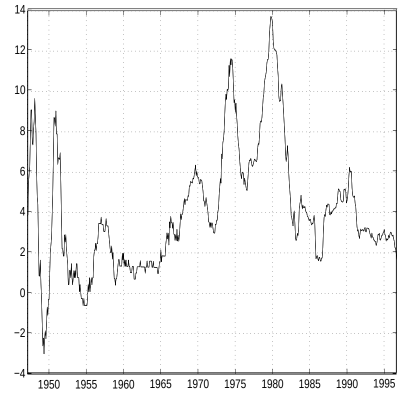

Figure 1: Moving average of monthly C.P.I. inflation, all items.

because the government temporarily has learned the natural rate hypothesis. The escapes occur via a remarkable type of dynamics reflecting accidental experimentation induced by the government's adaptive algorithm and its imperfect model. By focusing on a manageable special case, this paper obtains analytical characterizations of those escape dynamics.[1] Figure 1 shows the inflation rate in the U.S. consumer price index after World War II. It displays a rise in the late 1960's and 1970's, with a dramatic stabilization under Volcker around 1980, then a further reduction under Greenspan in the early 1990's.

We want to think about these data in terms of a model with the following features: (1) the monetary authority controls the inflation rate, apart from a random disturbance; (2) the true data generating mechanism embodies a version of the natural rate hypothesis embedded within an expectational Phillips curve; and (3) as in Kydland and Prescott (1977), a purposeful government dislikes inflation and unemployment and a private sector forecasts inflation optimally. An innovation of this paper is to add: (4) that the monetary policy makers don't know the true data generating mechanism but use a good fitting approximating model.

Within models with features (1), (2), and (3), there are two approaches to explaining the data in Figure 1. The first is the hypothesis of Parkin (1993) and Ireland (1997) that movements in the fundamentals of the basic Kydland-Prescott model caused the time-consistent inflation rate to vary over time, and that observed inflation tracked these movements. Parkin and Ireland assume fixed preferences and fixed beliefs for the policy authority and the public, but a shifting natural rate of unemployment.

The second approach posits that while the data from the 1970's may have tracked the time consistent inflation rate, after the early 1980's the monetary authorities chose infla-

[1]Since we completed this paper, we have received Williams (1999), which manages to compute the dominant escape route for a closely related model. Williams slightly modifies the learning algorithm by ignoring the R term below in order to simplify the analysis. He is able to obtain a diffusion approximation and to numerically minimize a version of the action functional to be described below. The dominant escape route computed by Williams closely resembles the one computed here.

tion below the time consistent rate. Some papers (e.g., Ball (1995)) have formalized this view in terms of particular specifications of history-dependent strategies for the monetary authorities that encode reputations. Others (e.g., McCallum (1995) and Blinder (1998)) suggest that the American monetary authorities have somehow, through unspecified means, managed to commit themselves to a better than time consistent inflation rate.

This paper contributes another theory within second approach. We hold fixed the fundamentals in the economy, including the true data generating mechanism, preferences, and agents' methods for constructing behavior rules. Changes in the government's beliefs about the Phillips curve, and how it approximates the natural rate hypothesis, drive the inflation rate. Inspired by econometric work about approximating models by Sims (1972) and White (1982), we endow the monetary authority, not with the correct model, but with an approximating model that it nevertheless estimates with good econometric procedures.

We use the concept of a self-confirming equilibrium, a natural equilibrium concept for behavior induced by an approximating model. Among the objects determined by a self-confirming equilibrium are the parameters of the government's approximating model. While the self-confirming equilibrium concept differs formally from a Nash (or time consistent) equilibrium,[2] it happens that the self-confirming equilibrium outcomes are the time-consistent ones. Thus, the time consistent outcome continues to be our benchmark.

Like a Nash equilibrium, a self-confirming equilibrium is stated in terms of population objects (mathematical expectations, not sample means). We add adaptation by requiring the government to estimate its model from historical data in real time. We form an adaptive model by having the monetary authority adjust its behavior rule in light of the latest model estimates. Thus, we attribute 'anticipated utility' behavior (see Kreps (1998)) to the monetary authority. Following Sims (1988), we study a 'constant gain' estimation algorithm that discounts past observations. Called a 'tracking algorithm', it is useful when parameter drift is suspected (see e.g. Marcet and Nicolini (1997)).

Results from the literature on least squares learning (e.g., Marcet and Sargent (1989), Woodford (1990), Evans and Honkapohja (1998)) apply and take us part way, but only part way, to our goal. The literature shows how the limiting behavior of systems with least squares learning is governed by a deterministic dynamics, described by an ordinary differential equation and known as 'mean dynamics'. These results imply that the adaptive system with least squares learning converges to the self-confirming equilibrium and the time consistent outcome. We go beyond the previous literature on least squares learning and discover another *deterministic* component of the dynamics that governs the system under the constant gain algorithm. These are the 'escape' dynamics. They point away from the self-confirming equilibrium and toward the Ramsey (or optimal-under-commitment) equilibrium outcome. So two sorts of dynamics dominate the behavior of the adaptive system.

1. The *mean dynamics* come from an unconditional moment condition, the least squares normal equations. These dynamics drive the system *toward* a self-confirming equilibrium.

[2] It is defined in terms of different objects.

2. The *escape route dynamics* propel the system *away* from a self-confirming equilibrium. They emerge from the same least squares moment conditions, but they are *conditioned* on a particular "most likely" unusual event, defined in terms of the disturbance sequence. This most likely unusual event is endogenous.

Under least squares adaptation without discounting of past observations, the mean dynamics dominate in the limit. They make the system converge to a self-confirming equilibrium. Under the adaptive system with constant gain, the escape route dynamics endure and occasionally drive the system *toward* the optimal (time inconsistent) outcome.

The escape route dynamics have a compelling behavioral interpretation. Within the confines of its approximate model, learning the natural rate hypothesis requires that the government generate a sufficiently wide range of inflation experiments. To learn even an imperfect version of the natural rate hypothesis, the government must experiment more than it does within the confines of a self-confirming equilibrium. The government is caught in an experimentation trap. With a constant gain, the adaptive algorithm occasionally puts enough movement into the government's beliefs to produce informative experiments.

1.1 Simplifications

Sargent (1999) studied these matters within the context of the distributed lag specification of the Phillips curve used in empirical applications. To simplify the approximation and control issues, this paper confines itself to a context in which the government estimates a static Phillips curve. This is the setting studied by Sims (1988). A cost of this simplification is that it eliminates important points about the "induction hypothesis" of Cho and Matsui (1995) and how distributed lag specifications of the Phillips curve can approximate the natural rate theory under particular experiments. A benefit is how the current setting illuminates the role of induced experimentation in promoting escapes from the time-consistent equilibria.

1.2 Related literature

Evans and Honkapohja (1993) investigated a model with multiple self-confirming equilibria having different rates of inflation. When agents learn through a recursive least squares algorithm, outcomes converge to a self-confirming equilibrium that is stable under the learning algorithm. When agents use a fixed gain algorithm, Evans and Honkapohja (1993) demonstrated that the outcome oscillates among different locally stable self-confirming equilibria. They suggested that such a model can explain wide fluctuations of market outcomes in response to small shocks.

In models like Evans and Honkapohja (1993), the time spent in a neighborhood of a locally stable equilibrium and the escape path from its basin of attraction are determined by a large deviation property of the recursive algorithm. As the stochastic perturbation disappears, the outcome stays in a neighborhood of a particular locally stable self-confirming equilibrium (exponentially) longer than the others. This observation provided Kandori, Mailath, and Rob (1993) and Young (1993) with a way to select a unique equilibrium in evolutionary models with multiple locally stable Nash equilibria.

An important difference from the preceding literature is that our model has a unique self-confirming equilibrium. Despite that, the dynamics of the model resemble those for models with multiple equilibria such as Evans and Honkapohja (1993). With multiple locally stable equilibria, outcomes escape from the basin of attraction of a locally stable outcome to the neighborhood of another locally stable equilibrium. The fact that our model has a globally unique stable equilibrium creates an additional challenge for us, namely, to characterize the most likely direction of the escape from a neighborhood of the unique self-confirming equilibrium. As we shall see, the most likely direction entails the government's learning a good, but not self-confirming, approximation to the natural rate hypothesis.

1.3 Organization

The remainder of this paper focuses on a learning mechanism that facilitates sufficient experimentation occasionally to offset the strong forces driving an adaptive system toward the pessimistic Kydland-Prescott time consistent equilibrium. Section 2 describes the basic setting. Section 3 defines and computes the Nash equilibrium and the Ramsey outcome. Section 4 defines a self-confirming equilibrium and shows how it supports a Nash outcome. Section 5 describes a minimal modification of a self-confirming equilibrium formed by giving the government an adaptive algorithm for its beliefs. In section 6, using simulations, we study how and why adaptation facilitates experimentation and escapes to better than time-consistent outcomes. Section 7 offers an economic interpretation of the escape path. Section 8 specializes the setting to multinomial shocks, for the sake of analytic tractability. In section 9, we formally examine the asymptotic properties of the escape path by investigating the large deviation properties of the underlying recursive learning algorithm. Section 10 discusses a more general setting and concludes. A final appendix gives a brief post World War II pictorial history of the U.S. Phillips curve.

2 Setup

We start with a framework and an idea of Sims (1988). We use Sims's version of Kydland and Prescott's model of a time-consistent government inflation policy and restate it in language used by Stokey (1989). First we form two rational expectations equilibria (Nash and Ramsey). Then we formulate a version of the model called a self-confirming equilibrium. Here the government uses an approximating model. After that, we describe our main interest, an adaptive version of the model in which the government fits its approximating model using a recursive algorithm that discounts past observations.

Let $(U_t, y_t, x_t, \hat{x}_t)$ denote the unemployment rate, the inflation rate, the systematic part of the inflation rate, and the public's expected rate of inflation, respectively. The government sets x_t, the public sets $\hat{x}_t$, and the economy determines outcomes (y_t, U_t).

2.1 The Private Economy

The data are generated by the natural unemployment rate model

$$\begin{aligned} U_t &= U^* - \theta(y_t - \hat{x}_t) + v_{1t} && (2.1)\\ y_t &= x_t + v_{2t} && (2.2)\\ x_t &= \hat{x}_t, && (2.3) \end{aligned}$$

where $\theta > 0$, $U^* > 0$, and v_t is a (2×1) i. i. d. random vector with $Ev_t = 0$, diagonal contemporaneous covariance matrix and $Ev_{jt}^2 = \sigma_{vj}^2$. Here U^* is the natural rate of unemployment and $-\theta$ is the slope of an expectations-augmented Phillips curve. According to (2.1), there is a family of Phillips curves indexed by $\hat{x}_t$. Condition (2.2) states that the government sets inflation up to a random term v_{2t}. Condition (2.3) imposes rational expectations for the public. System (2.1), (2.2), (2.3) embodies the natural unemployment rate hypothesis: surprise inflation lowers the unemployment rate but anticipated inflation does not.

2.2 The government's purpose

The government has a preference ordering over (y_t, U_t) induced by the one-period return function

$$-E(U_t^2 + y_t^2). \tag{2.4}$$

3 Equilibria with knowledge of model

The literature focuses on two equilibria that arise from assuming that the government knows the correct model. Called the Nash equilibrium and the Ramsey plan, they come from different timing protocols. The outcome with a Ramsey plan is better than that for a Nash equilibrium. This is the time inconsistency problem.

To define a Nash equilibrium, we need

Definition 3.1 *A government* best response *map* $x_t = B(\hat{x}_t)$ *solves the problem*

$$\min_{x_t} E(U_t^2 + y_t^2) \tag{3.5}$$

subject to (2.1), (2.2), taking $\hat{x}_t$ *as given.*

The best response map is

$$x_t = \frac{\theta}{\theta^2 + 1} U^* + \frac{\theta^2}{\theta^2 + 1} \hat{x}_t. \tag{3.6}$$

A Nash equilibrium incorporates a government best response and rational expectations for the public:

Definition 3.2 *A* Nash equilibrium *is a pair* $(x, \hat{x})$ *satisfying (a)* $x = B(\hat{x})$*, and (b)* $\hat{x} = x$*. A* Nash outcome *is the associated* (U_t, y_t).

Definition 3.3 *The* Ramsey plan x_t *solves the problem of minimizing (3.5) subject to (2.1), (2.2), and (2.3). The* Ramsey outcome *is the associated* (U_t, y_t).

A Ramsey outcome dominates a Nash outcome. The Ramsey plan is $\hat{x}_t = x_t = 0$ and the Ramsey outcome is

$$U_t = U^* - \theta v_{2t} + v_{1t}, \quad y_t = v_{2t}. \tag{3.7}$$

The Nash equilibrium is $\hat{x}_t = x_t = \theta U^*$ and the Nash outcome is $U_t = U^* - \theta v_{2t} + v_{1t}, y_t = \theta U^* + v_{2t}$. The addition of constraint (2.3) to the government's problem in the Ramsey plan makes the government achieve better outcomes by taking into account how its actions affect the public's expectations. The superiority of the Ramsey outcome reflects the value to the government of being able to commit to a policy before the public sets its expectations. This is how Kydland and Prescott (1977) reached the pessimistic conclusion that a benevolent and knowledgeable government would set inflation too high because it makes decisions sequentially, not once-and-for-all time.

4 Equilibrium with an approximating model

Following Sims (1988), we now study a setting where the government does not know the structure and makes policy with an econometric model that approximates the economy. This leads to a model with two models within, one the true model (2.1), (2.2), (2.3), the other the government's econometric model.

In particular, the government does not know (2.1) and (2.3), but believes (2.2) and

$$U_t = \gamma_0 + \gamma_1 y_t + \epsilon_t, \tag{4.8}$$

where ϵ_t is a random variable orthogonal to the constant and y_t, which makes (4.8) a regression equation. Specification (4.8) ignores the hidden state $\hat{x}_t$ that truly positions the Phillips curve in (2.1). The government's beliefs are restricted by the least-squares normal equation

$$E\epsilon_t \begin{bmatrix} 1 \\ y_t \end{bmatrix} = 0, \tag{4.9}$$

where E is the mathematical expectation operator; (4.9) identifies γ as a population least squares regression vector. Equation (2.2) continues to express the government's belief that it can control y_t up to a random term.

4.1 The government's decision problem

Substituting (2.2) into (4.8) gives

$$U_t = \gamma_0 + \gamma_1(x_t + v_{2t}) + \epsilon_t. \tag{4.10}$$

We use

Definition 4.1 *A government* pseudo best response *map* $x_t = h_o(\gamma)$ *solves*

$$\min_{x_t} E(U_t^2 + x_t^2) \tag{4.11}$$

subject to (4.10).

The pseudo best response is

$$x_t = \frac{-\gamma_0\gamma_1}{\gamma_1^2 + 1} \equiv h_o(\gamma). \tag{4.12}$$

It maps an approximating Phillips curve γ into the government's setting of the systematic part of inflation x_t.

4.2 Self-confirming equilibrium

Definition 4.2 *A* self-confirming equilibrium *is a government belief* γ*, a government pseudo best response map for* x_t*, and an associated stochastic process for* $(U_t, y_t, x_t, \hat{x}_t)$ *such that: (a) the stochastic process satisfies (2.1), (2.2), (2.3); (b)* x_t *satisfies (4.12); (c) the regression coefficients* γ *satisfy (4.9).*

Condition (a) requires that the data are generated by the true model and that the public's expectations are rational. Condition (b) requires that the government set the systematic part of inflation to be a pseudo best response to its beliefs about the Phillips curve. Condition (c) requires that the government's beliefs about the Phillips curve be consistent with the data.

Proposition 4.3 *The self-confirming equilibrium outcome equals the Nash outcome.*

Proof: We proceed by constructing the self-confirming equilibrium outcome and comparing it to the Nash outcome. To compute a self-confirming equilibrium, substitute rule (4.12) and (2.3) into (2.1) to get

$$U_t = [U^* + h_o\theta] - \theta y_t + v_{1t}. \tag{4.13}$$

Equating coefficients in (4.13) and (4.8) and rearranging gives γ in a self-confirming equilibrium:

$$\gamma_1 = -\theta \tag{4.14}$$

$$\gamma_0 = U^*(1 + \theta^2). \tag{4.15}$$

Substituting these values into (4.12) gives

$$x_t = \theta U^*. \tag{4.16}$$

This equals the setting for x_t under a Nash equilibrium. *Q.E.D.*

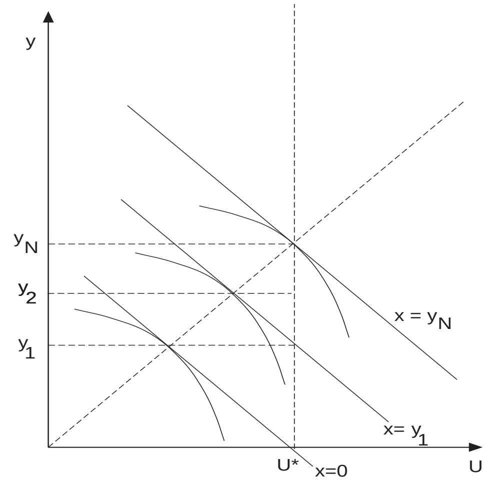

Figure 2: Nash and Ramsey outcomes and best response expansion path.

Within a self-confirming equilibrium, the moment matrix of the variables on the right of the government's regression (4.8) satisfies

$$R \equiv M(\gamma) = E \begin{bmatrix} 1 \\ y_t \end{bmatrix} [1 \;\; y_t] = \begin{bmatrix} 1 & h_o(\gamma) \\ h_o(\gamma) & h_o(\gamma)^2 + \sigma_2^2 \end{bmatrix}, \tag{4.17}$$

where γ is evaluated at self-confirming equilibrium values (4.14), (4.15).

4.3 Source of suboptimality

In the self-confirming equilibrium, the government's approximating model correctly captures the short-run Phillips curve trade-off between U_t and y_t, although it fails to identify the role of the expected inflation rate $\hat{x}_t$ in positioning the Phillips curve. See figure 2, adapted from Kydland and Prescott (1977). In a self-confirming equilibrium, the estimated Phillips curve coincides with the true Phillips curve evaluated at the Nash equilibrium value of expected inflation. The effects of expected inflation $\hat{x}$ are absorbed into the constant γ_0. Since x_t and $\hat{x}_t$ are constant in the self-confirming equilibrium, the failure to identify $\hat{x}$ as a shifter costs the government nothing in terms of statistical fit. The self-confirming equilibrium is suboptimal because the Nash equilibrium is suboptimal.

It is useful to find the parameter values that would induce the government to implement the Ramsey inflation policy $x_t = 0$. From the pseudo-best response map (4.12), the government must believe that $\gamma_1 = 0$ if it is to set $x_t = 0$: it must believe that the Phillips curve is vertical. But the Phillips curve is not vertical in a self-confirming equilibrium. The empirical Phillips curve (4.8) *would* be approximately vertical had the government and the public experimented by setting $x_t = \hat{x}_t$ randomly over a sufficiently wide set of values. However, within a self-confirming equilibrium, the government and the public set

$x_t = \hat{x}_t = x_N$, the suboptimal constant Nash equilibrium value, and the government's estimate of γ_1 becomes $-\theta$.

5 An adaptive system

Following Sims (1988), we now make a minimal modification of the preceding model of self-confirming equilibrium with an approximating model. We withdraw knowledge of the population parameters γ_0, γ_1, and instead endow the government with a recursive algorithm for estimating those parameters from historical data. The recursive estimation algorithm is a version of least squares. Each period, the government sets x_t by substituting its most recent estimate of γ into its behavior rule (4.12). Thus, we posit that the government behaves each period as though its estimate of γ were known and permanent, even though it updates that estimate in response to new data.[3] This leads to an anticipated utility model (Kreps (1997)) for the government. The specification generates data from a version of (2.1), where

$$x_t = h_o(\gamma_t) \tag{5.18}$$

and where $h_o(\gamma)$ continues to satisfy (4.12). We assume that $\hat{x}_t = x_t$, so that "Fed watchers" tell the private sector the government's behavior rule.[4] Augmenting (2.1), (2.2), (2.3), (5.18), (4.12) with an adaptive formula for γ_t completes the model. We express the learning rule for γ in the recursive form

$$\begin{aligned}
\begin{bmatrix} \gamma_{0t+1} \\ \gamma_{1t+1} \end{bmatrix} &= \begin{bmatrix} \gamma_{0t} \\ \gamma_{1t} \end{bmatrix} + a_t R_t^{-1} \begin{bmatrix} 1 \\ y_t \end{bmatrix} (U_t - \gamma_{0t} - \gamma_{1t} y_t) && (5.19) \\
R_{t+1} &= R_t + a_t \left(\begin{bmatrix} 1 \\ y_t \end{bmatrix} [1 \quad y_t] - R_t \right). && (5.20)
\end{aligned}$$

where $\{a_t\}$ is a sequence of positive real numbers and R_t is an estimate of the moment matrix of $\begin{bmatrix} 1 \\ y_t \end{bmatrix}$. The second term on the right of (5.19) is a weighting matrix times the time t value of the least squares orthogonality condition for the government's Phillips curve γ. The algorithm adjusts γ in a direction to make the orthogonality condition hold, not on average, but for this period's shock. Setting $a_t \sim t^{-1}$ recovers a version of least squares. We shall be interested in constant gain algorithms where $a_t = a$ for all t. Compared to least squares, an algorithm with a constant a discounts past observations.

This leads to the following data generating mechanism:

$$\begin{bmatrix} \gamma_{0t+1} \\ \gamma_{1t+1} \end{bmatrix} = \begin{bmatrix} \gamma_{0t} \\ \gamma_{1t} \end{bmatrix} + a_t R_t^{-1} \begin{bmatrix} 1 \\ y_t \end{bmatrix} (U_t - \gamma_{0t} - \gamma_{1t} y_t) \tag{5.21}$$

[3] The government does not experiment intentionally, and does not proceed as advocated by Wieland (1997).

[4] We would get similar data patterns if we instead gave the private sector agents their own recursive algorithm for forecasting inflation with a gain parameter equal to the government's.

$$
\begin{aligned}
R_{t+1} &= R_t + a_t\left(\begin{bmatrix} 1 \\ y_t \end{bmatrix}[1 \quad y_t] - R_t\right). && (5.22)\\
x_t &= h_o(\gamma_t) = \frac{-\gamma_{1,t}\gamma_{0,t}}{1+\gamma_{1t}^2} && (5.23)\\
y_t &= x_t + v_{2t} && (5.24)\\
U_t &= U^* - \theta v_{2t} + v_{1t}. && (5.25)
\end{aligned}
$$

Here (γ, R) summarize the government's beliefs.

6 An associated o.d.e. and mean dynamics

The analysis of convergence of least squares in self-referential systems in Marcet and Sargent (1989) and Woodford (1990) rests on results from stochastic approximation theory. They approximate the limiting behavior of the stochastic system with an o.d.e. This paper will extend this analysis by finding another o.d.e. that governs expulsions away from a self-confirming equilibrium.

To prepare to find these o.d.e.'s, write (5.19) more compactly as

$$\gamma_{t+1} = \gamma_t + a_t b(\gamma_t, v_t) = \gamma_t + a_t \begin{bmatrix} b_0(\gamma_t, v_t) \\ b_1(\gamma_t, v_t) \end{bmatrix} \tag{6.26}$$

and $v_t = (v_{1t}, v_{2t})$. A straightforward calculation shows that

$$b(\gamma_t, v_t) = R^{-1}\begin{bmatrix} 1 \\ x_t + v_{2t} \end{bmatrix} z(\gamma_t, v_t) \tag{6.27}$$

where

$$z(\gamma, v_t) = U^* - \frac{\gamma_0}{1+\gamma_1^2} + v_{1t} - (\theta + \gamma_1)v_{2t}. \tag{6.28}$$

Notice that $z(\gamma, v)$ is the residual ϵ in the government's Phillips curve (4.8). When we drop time subscripts, we shall mean the continuous time counterpart of the variables in the corresponding discrete time variable. The *mean dynamics* are

$$
\begin{aligned}
\dot{\gamma} &= \bar{b}(\gamma) = R^{-1}\begin{bmatrix} U^* - \frac{\gamma_0}{1+\gamma_1^2} \\ -\frac{\gamma_0\gamma_1}{1+\gamma_1^2}\left(U^* - \frac{\gamma_0}{1+\gamma_1^2}\right) - \sigma_2^2(\theta+\gamma_1) \end{bmatrix} && (6.29)\\
\dot{R} &= M(\gamma) - R, && (6.30)
\end{aligned}
$$

where $M(\gamma)$ is from (4.17). This is the associated o.d.e. used by Marcet and Sargent (1989) and Woodford (1990) to analyze related models. The o.d.e. (6.29) is derived by taking the unconditional[5] mean of $b(\gamma, v)$, the term multiplying a_t in (6.26). The o.d.e. (6.30) is derived in a similar way from (5.20). The o.d.e. (6.29), (6.30) has a unique stable point $\gamma^s = (-\theta, U^*(1+\theta^2))$, the γ associated with a self-confirming equilibrium. Let R^s be the associated fixed point of (6.30).

[5] Later we shall find other o.d.e.'s derived by averaging the shocks in (6.26) with respect to other distributions.

6.1 Self-confirming equilibrium as unconditional moment conditions

The right side of (6.29) incorporates three aspects of the model: (1) the time t value of the least squares orthogonality conditions for the government's estimator of γ; (2) the government's pseudo-best response in setting $\hat{x}_t$ as a function of γ; and (3) the true Phillips curve and inflation generating mechanism (2.1), (2.2), (2.3). Together, these form a differential equation whose right side, when equated to zero, can be interpreted as a set of unconditional moment restrictions that determines a self-confirming equilibrium. The mean dynamics are interesting because they determine the limiting behavior of the stochastic discrete time algorithm when a_t eventually behaves as $\frac{1}{t}$, as it does under least squares. More precisely, by applying results of Marcet and Sargent (1989) and Woodford (1990), we can show that if the gain a_t is equal to a_0/t for $t \geq 1$, then $\gamma_t \to \gamma^s$ with probability 1. We summarize this in

Proposition 6.1 *If the adaptive system under least squares converges, it converges almost surely to a self-confirming equilibrium. Further, because the mean dynamics are globally stable, global convergence obtains once the algorithm is modified to prevent it from wandering outside a given neighborhood of the self-confirming equilibrium.*

Marcet and Sargent (1989) and Evans and Honkapohja (1998) describe conditions on the recursive algorithm that suffice. The crudest of these is borrowed from Ljung (1977) and uses a projection facility to force (γ, R) to remain in the domain of attraction of (γ^s, R^s).

To sustain outcomes other than the self-confirming equilibrium outcome in the limit, we must arrest Proposition 6.1. We shall do so in an economical way that retains the basic spirit of least squares learning in self-referential models.

Thus, the idea behind least squares learning (e.g., Evans and Honkapohja (1999)) is to endow agents with a statistical model that might be "wrong" during a transition, but that has a chance of eventually being "correct" should convergence occur. Typically, the reason that agents' models are wrong during transitions is that they are fixed-coefficient models, while agents' estimation procedures and behaviors in the aggregate cause the coefficients in truth to drift. Eventually, however, things may settle down so that the fixed-coefficients assumption becomes correct. The problem posed by Bray (1982) was to establish convergence to a correct (i.e., rational expectations) specification of a particular sequence of incorrect specifications induced by least squares learning. The mean dynamics are a good way to study this problem. See Woodford (1990) and Marcet and Sargent (1989).

The $a_t = \frac{a_0}{t}$ specification implicitly embodies the fixed-coefficient misspecification of least squares. During a transition, an agent would improve forecasts were he to copy practitioners who, when confronted with drifting coefficients, discount past observations. Discounting makes sense if the model being estimated has coefficients that are random walks. In particular, there is a Bayesian formulation of Gaussian random walk coefficients that leads to a constant gain algorithm. See Sargent (1999).

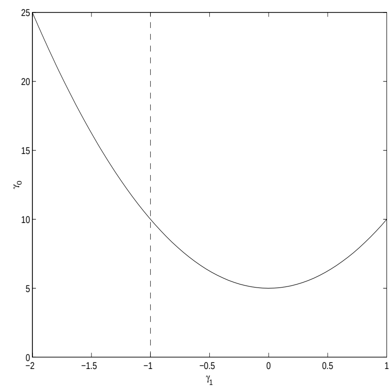

Figure 3: Self-confirming equilibrium with $U^* = 5, \theta = 1$.

6.2 Simulations: evidence for another o.d.e.

In the next section, we present some simulations that show the mean dynamics at work but that also indicate another nearly deterministic kind of dynamics. This other source of dynamics looks like it is solving *some* o.d.e., but not the mean dynamics. The rest of the paper seeks this other o.d.e. The source of this o.d.e. must be the original system (5.21), (5.22), (5.23), (5.24), (5.25). We shall see that the new o.d.e. comes from the same moment conditions as the mean dynamics, with expectations being conditioned on an endogenous sequence of unusual shocks.

6.3 Simulations

We are interested in the behavior exhibited by the system in the constant gain case $a_t = a$ for $\forall t \geq 1$. We will display some simulations that show the workings of two distinct sources of dynamics: the mean dynamics associated with (6.29), and some "escape route dynamics" that are activated when the government engages in enough experimentation to make it learn (too strong) a version of the natural rate hypothesis.

The simulations are from a version of the algorithm (5.21), (5.22), (5.23), (5.24), (5.25). For the simulations, we set $\theta = 1, U^* = 5$. We assumed Gaussian disturbances. We set $(\sigma_1, \sigma_2) = (.3, .3)$ in the first simulation and $(.5, .5)$ in the second. The definition of $\bar{b}(\gamma)$ in (6.29) shows the self-confirming equilibrium to be the intersection of the line $\gamma_1 = \theta$ with the parabola determined by $U - \frac{\gamma_0}{1+\gamma_1^2} = 0$. There is a unique self-confirming equilibrium, depicted in Figure 3. It has $\gamma_0 = 10, \gamma_1 = -1$.

Figures 4 and 5 display aspects of the two simulations. The mean inflation rate in a self-confirming equilibrium is 5. The mean inflation in the Ramsey equilibrium is 0. Notice that from (4.12), the government would set the systematic part of inflation at the Ramsey level of 0 only if it believed that the Phillips curve is vertical ($\gamma_0 = 0$).

We initiated each simulation from a self-confirming equilibrium and set a constant gain parameter $a = .0275$.[6] The first three panels in Figures 4 and 5, respectively, show the rate of inflation, γ_{1t}, and the time t variance of γ_{1t}. The fourth panels of Figures 4 and 5 display scatter graphs of $(\gamma_{0t}, \gamma_{1t})$, together with a solid line that indicates the locus of (γ_1, γ_0) that solve $U^* = -\frac{\gamma_0}{1+\gamma_1^2}$. The simulations show:

1. Usually, the adaptive system follows a noisy version of the mean dynamics $\bar{b}(\gamma)$ and heads toward a self-confirming equilibrium. This reflects the workings of the usual Woodford-Marcet-Sargent convergence theorems. For σ_2 small (as we have set it), the mean dynamics of $\bar{b}(\gamma)$ lie virtually along the parabola $U^* = \frac{\gamma_0}{1+\gamma_1^2}$ (see the definition of $\bar{b}$ associated with (6.29)). The simulations show γ_1, γ_0 paths adhering closely to this parabola during the typical episodes heading toward the self-confirming equilibrium. For γ_1, γ_0 on the parabola and $\gamma_1 > -\theta$, notice that the mean dynamics of $\bar{b}$ from (6.29) have $\frac{d}{dt}\gamma_0 = 0, \frac{d}{dt}\gamma_1 < 0$. This explains why most of the points near the parabola cluster slightly underneath the parabola.

2. There are occasional recurrent rapid movements away from a self-confirming equilibrium toward a neighborhood of the Ramsey inflation outcome. These rapid movements do not simply reverse direction and follow the mean dynamics path $(\gamma_1, \gamma_1) \in \Re^2$ away from a self-confirming equilibrium. They take another shorter (in some sense) route. The "escape routes" are almost straight lines in (γ_1, γ_0) space toward the Ramsey outcome.

3. The sample variance of the estimated parameter γ_1 typically grows along the dynamic path heading toward the self-confirming equilibrium, then collapses during the escape to near Ramsey.

6.4 The escape route

For the same set of parameter values with $\sigma_1 = \sigma_2 = .3$, we ran many simulations to learn more about the escape route. We used the simulations to estimate the distribution of escape routes and the time to first escape. Starting from a self-confirming equilibrium, each simulation runs for a random number of periods. The stopping time for a simulation was determined by the event that the government set the target inflation rate at a level within $\delta = .75$ of the Ramsey inflation outcome. For each sample path, we then recorded the path of beliefs $(\gamma_{1t}, \gamma_{0t})$ to the neighborhood of the Ramsey outcome and the number of periods that elapse from the beginning of the simulation to the event that the government's beliefs prompt it to enter the prescribed neighborhood of the Ramsey outcome. Figures 6 and 7 describe these statistics for large numbers of simulated paths. Figure 6 plots 500 escape paths, and Figure 7 plots the histogram of first passage time to the neighborhood of the Ramsey for 5000 sample paths. We plot only 500 escape paths to contain the size of the

[6] See Appendix B to chapter 8 of Sargent (1999) for the connection between a and a discount parameter in a loss function.

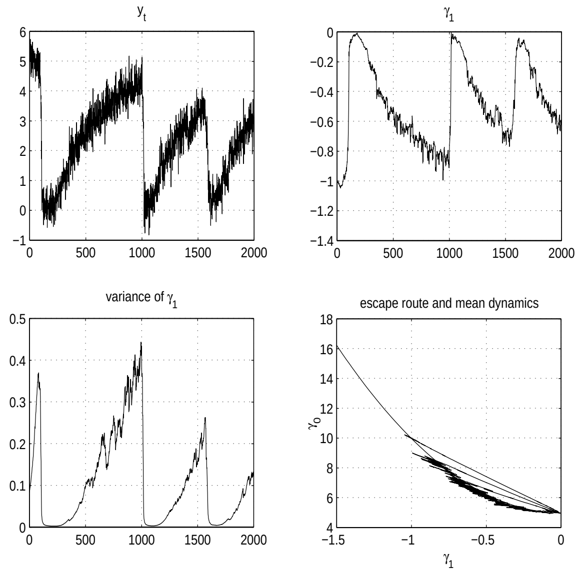

Figure 4: Simulation with constant gain, $\sigma_1 = \sigma_2 = .3$.

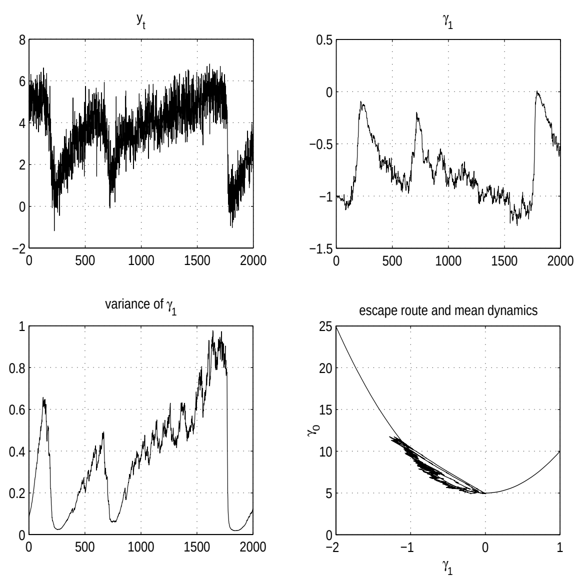

Figure 5: Simulation with constant gain, $\sigma_1 = \sigma_2 = .5$.

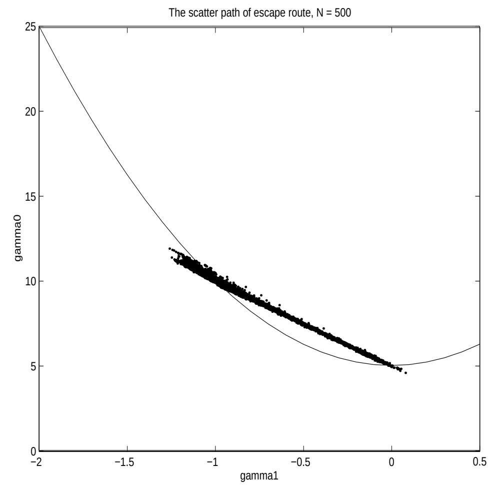

Figure 6: Scatter of 500 escape routes, $a = .0275$.

postscript file that generates the graph. With 5000 points, the escape route graph is only a little thicker and centered on the same route. For the sample of 5000 sample paths, the mean time of transition to a neighborhood of Ramsey is 49.3 with a standard deviation of 36.2 and a median of 38.

Other simulations with lower constant values of a reveal the same escape route but have distributions of escape times to the Ramsey neighborhood that are shifted to the right relative to Figure 7.

The striking feature of Figure 6 is how tightly bunched are the paths of beliefs moving from the vicinity of the self-confirming equilibrium to the neighborhood of Ramsey. This reflects the "near determinism" that Whittle (1996) tells us about escape route dynamics. We can summarize the dynamics of escapes to Ramsey in the following rough phrase: escapes to Ramsey are unusual events; but given that they occur, with high probability they occur nearly along the most likely path.[7] We explain this mysterious phrase in the context of the special case that v_{it} is binomial for $i = 1, 2$.[8] But first we briefly interpret the escapes from the self-confirming equilibrium in terms of the behavior of the government.

7 Escaping the experimentation trap

The striking feature of the simulations is the large and rapid departures from the self-confirming equilibrium that always approach the Ramsey outcome along a common escape route. Notice how the slope coefficients go rapidly nearly to zero during the stabilization. What prompts the stabilizations is a chance process through which the government

[7]We are paraphrasing Michael Harrison's verbal account of one of the two fundamental results of large deviation theory.

[8]For binomial shocks we have obtained simulations that are qualitatively the same as those reported above.

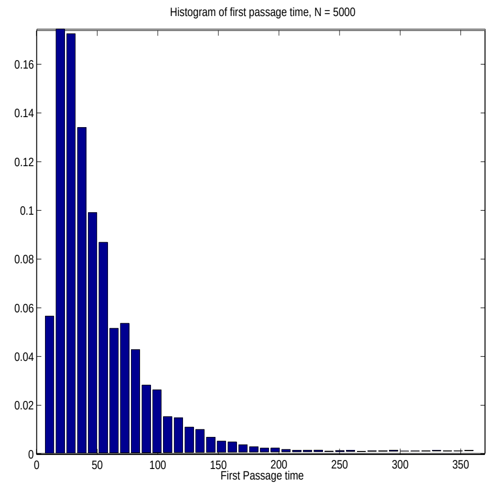

Figure 7: Histogram of 5000 first escapes to neighborhood of Ramsey.

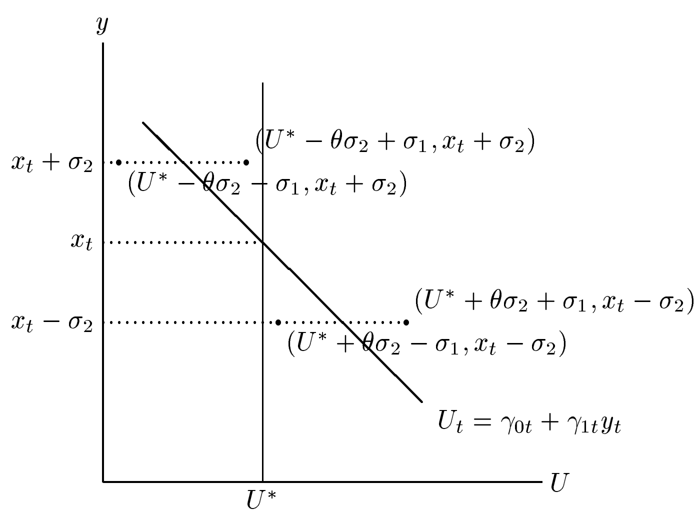

Figure 8: Estimated Phillips Curve and four possible realizations of outcome (U_t, y_t) in period t.

learns a stronger-than-is-true version of the natural unemployment rate hypothesis (the government doesn't distinguish between surprise and anticipated inflation).

In a self-confirming equilibrium, the government is in an experimentation trap. Within the confines of the government's approximating model, detecting the natural rate hypothesis requires that there be sufficient dispersion in the public's expected rate of inflation. But within a self-confirming equilibrium, there is *no* variation in the expected rate of inflation because the government does not vary its setting of the systematic part of inflation x_t. Though the outcome is the same, the structure of this expectations trap differs from the one in Kydland and Prescott's time consistent equilibrium. Here the government fails to generate the range of experiments needed to detect the natural rate hypothesis within its approximating model. But only if it detects something approximating the natural rate hypothesis will it want to generate those experiments.

The escape route has the government generating those experiments because its doubts leave it open enough occasionally to experiment and to learn. The experiments are initiated by some unusual shock patterns that we shall analyze in detail below. The escapes to near the Ramsey outcome are accompanied by endogenous experimentation. Any force that causes the government to experiment by randomizing x_t generates a (y_t, U_t) data scatter through (2.1) that *steepens* (in the (y, U) plane) the estimated Phillips curve (4.8). Through (4.12), any steepening of the Phillips curve causes the government to lower inflation, generating influential observations to steepen the Phillips curve further. Overweighting recent observations helps this process along. This reinforcing process comes to a halt when the estimated Phillips curve (4.8) becomes vertical. The system cannot remain at the Ramsey outcome forever, because there is in truth a short-run Phillips curve that the government will discover and begin to exploit, rekindling the mean dynamics that drive the system toward the Nash outcome.

The simulations indicate that there is another nearly deterministic component of the dynamics that supplements the mean dynamics. We now seek them in a special case that permits us to get our arms around the escape route.

The explanation in terms of endogenous experimentation will be strengthened and formalized by the analysis of the following section where we find an o.d.e. that describes the escape route.

8 Binomial shocks

We shall analyze the multinomial case, but to simplify in the beginning we assume that v_{it} has a binomial distribution with variance σ_i^2 $(i = 1, 2)$:

$$v_{it} = \begin{cases} \sigma_i & \text{with probability } \frac{1}{2} \\ -\sigma_i & \text{with probability } \frac{1}{2}. \end{cases} \tag{8.31}$$

We proceed by studying in detail the structure of the orthogonality conditions that define self-confirming equilibrium and, what is the same thing, a fixed point of the government's learning scheme under least squares. Above, we have defined $z(\gamma, v_t)$ as the residual in the government's Phillips curve for regression coefficients γ and shock vector v_t. We expressed the least squares orthogonality conditions as

$$ER^{-1}\begin{bmatrix}1\\ y_t\end{bmatrix}z(\gamma, v_t) = 0$$

or

$$Eb(\gamma, v_t) = 0,$$

where the mathematical expectation is taken with respect to the unconditional distribution of v_t. The mean dynamics for γ were derived by setting

$$\dot{\gamma} = Eb(\gamma, v_t). \tag{8.32}$$

The escape dynamics occur when the algorithm is driven by a particular unusual sequence of v_t's. An associated o.d.e. that describes them comes from replacing E in (8.32) with an expectation operator conditioned on a particular draw of shocks.

Thus, let $\sigma \in \{\sigma_1, -\sigma_1\} \times \{\sigma_2, -\sigma_2\}$ be a realization of v_t. Since v_t can take four different values, for any $\gamma \in \Re^2$, $\{b(\gamma, v_t)\}$ consists of four vectors for any $\gamma \in \Re^2$. Let $R_t = [R_{ij,t}]$ and D_t be the determinant of R_t. We can write (6.26) as

$$\begin{bmatrix}\gamma_{0t+1}\\ \gamma_{1t+1}\end{bmatrix} = \begin{bmatrix}\gamma_{0t}\\ \gamma_{1t}\end{bmatrix} + a\frac{1}{D_t}\begin{bmatrix}R_{22,t} - R_{12,t}(x_t + v_{2,t})\\ -R_{12,t} + (x_t + v_{2,t})\end{bmatrix} z(\gamma_t, v_t). \tag{8.33}$$

Then from (8.33)

$$\frac{d\gamma_{0,t+1}}{d\gamma_{1,t+1}} = \frac{R_{22,t} - R_{12,t}(x_t + v_{2,t})}{-R_{12,t} + (x_t + v_{2,t})} \tag{8.34}$$

is independent of v_{1t}, which implies that for any v_t, $\{b(\gamma_t, v_t)\}$ consists of two pairs of linearly dependent vectors, each pair being indexed by one of the two possible values for v_{2t}. This fact is critical in shaping the escape route.

In (6.27), $b(\gamma, v_t) = 0$ if $z(\gamma, v_t) = 0$. For later analysis, it is useful to depict the contour of γ satisfying

$$z(\gamma, v_t) = 0$$

for each realization of v_t. As depicted in Figure 9, for example, $\gamma^{1,e}$ is the intersection of

$$\{\gamma : z(\gamma, (\sigma_1, \sigma_2)) = 0\}$$

and

$$\{\gamma : z(\gamma, (-\sigma_1, -\sigma_2)) = 0\}.$$

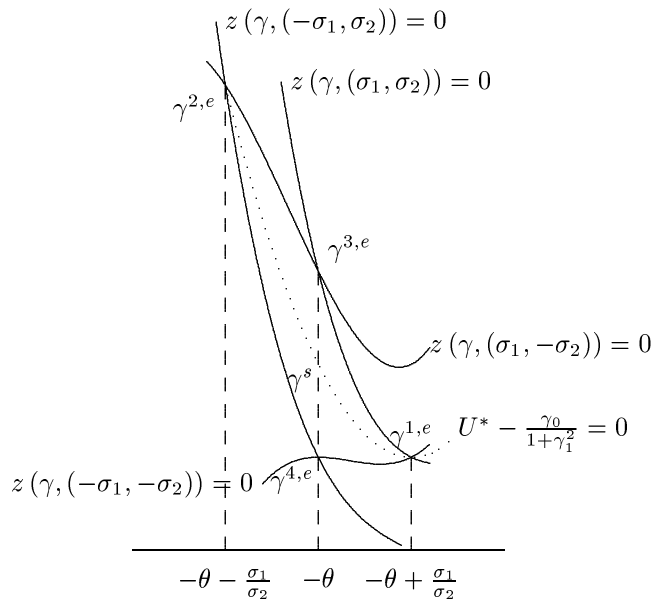

Figure 9: Stable solution γ^s and four "extreme" points $\gamma^{i,e}$ $(i = 1, \ldots, 4)$ with the boundary functions. The line connecting the four "extreme" points is the boundary of $\mathcal{D}^o$ which contains γ^s in the interior. The dotted curve passing through γ^s solves $\overline{b}_0(\gamma) = 0$.

9 The Escape Path

9.1 Introduction

We proceed by studying the dynamics when the amount of noise in the recursive stochastic system is very small.[9] Roughly speaking, as the noise in the recursive stochastic system disappears, the asymptotic behavior of the recursive algorithm can be approximated by the mean dynamics. Since the mean dynamics of the recursive system converges to the stable point, it is sensible to focus on the dynamics of γ_t around the stable point.

While the mean dynamics push γ_t toward the stable solution of the associated ordinary differential equation, the stochastic perturbation, albeit small, sometimes pushes γ_t away from the neighborhood of the stable solution. Our objective is to characterize the most likely path that γ_t follows while escaping from the neighborhood. We call it the *dominant escape path* (Bucklew (1990)).

Let $\mathcal{D}$ be an open ball around stable point of the mean dynamics γ^s. We follow the convention of fixing the starting point of the escape path at the stable solution γ^s and the terminal point $\gamma^e \in \partial\mathcal{D}$. In order to distinguish the path *converging to* γ^s from the path *escaping from* γ^s, we write the escape path as φ. Define the exit time τ^e as

$$\inf\{\tau \geq 0 : \varphi(\tau) = \gamma^e\}.$$

There are many escape paths starting from the same point. These paths are determined by the different $\{v_t\}$ sequences in (6.26) that succeed in driving γ to $\partial\mathcal{D}$. These paths pass through different points of the boundary of $\mathcal{D}$. Consequently, associated with the exit time is a probability distribution along the boundary of $\mathcal{D}$, induced by the probability distribution of the escape paths. As the gain sequence a converges to 0, however, the probability that a particular point in $\partial\mathcal{D}$ becomes an exit point is completely determined by the probability that the shortest escape paths through the point is realized. (This is the meaning of the mysterious phrase of Michael Harrison cited above.)

As $a \to 0$, the recursive system converges to a deterministic system in a probabilistic sense and the probability distribution of exit times converges to a degenerate distribution concentrated at the exit point of the dominant escape path. Thus, if φ is the dominant escape path, then for any $\mu > 0$, the shortest escape paths must converge to the μ neighborhood of φ with probability 1 as the gain sequence a converges to 0.

9.2 Key idea

From standard results of stochastic approximation, we know that as $a \downarrow 0$, the sample paths generated by a stochastic recursive algorithm converge to the mean dynamics with probability 1 over any finite time interval. As the gain sequence becomes smaller, the sample paths accumulate in a small neighborhood of the mean dynamics so that its neighborhood is the most likely location of a sample path. This observation suggests that the dominant

[9] Also known as a nearly deterministic system in Whittle (1996) or a system with small noise in Freidlin and Wentzell (1984).

escape path is characterized by a mean dynamics of *some* stochastic recursive algorithm. We now find that recursive algorithm. It is intimately connected to the original recursive algorithm (6.27) for γ_t.

9.3 Definitions

Because the notion of an escape path is built upon a continuous time process while the original recursive algorithm is a discrete time process, we need more notation. We shall use φ with various sub and superscripts to represent the escape path.

We borrow some notation from Kushner and Clark (1978). Define real time in terms of the gain sequence a:

$$t_k = ak$$

and $\forall \tau \in \Re_+$, there exists a unique k such that

$$\tau \in [t_k, t_{k+1}).$$

Define

$$m(\tau) = k.$$

Following the convention, let

$$\varphi_0^a = \gamma^s$$

and define

$$\varphi_{t+1}^a = \varphi_t^a + ab(\varphi_t^a, v_t) \tag{9.35}$$

where b is defined as (6.26). Except that φ_t^a takes the place of γ_t, (9.35) emulates the original recursive formula. However, we shall modify the probability distribution of v_t to push φ_t^a *away* from the initial point γ^s and toward $\partial\mathcal{D}$. Let $\varphi^a(\tau)$ be the continuous time process obtained by linearly interpolating φ_t^a, and let $\varphi_\tau^a(s)$ be the left shift of $\varphi^a(\tau + s)$.

Definition 9.1 *φ^a is an escape path from $\gamma^s \in \mathcal{D}$ if φ^a is absolutely continuous, $\varphi^a(0) = \gamma^s$ and*

$$\tau^e = \inf\{\tau \geq 0 : \varphi^a(\tau) \notin \mathcal{D}\} < \infty.$$

We call τ^e the escape time, and $\varphi^a(\tau^e)$ the exit point. φ^a is the shortest escape path to $\gamma^e \in \partial\mathcal{D}$ if φ^a is an escape path satisfying $\varphi^a(\tau^e) = \gamma^e$ and among all escape paths that exit $\mathcal{D}$ through γ^e, τ^e is the minimal escape time.

The exit time τ^e is associated with a probability distribution along $\partial\mathcal{D}$. To emphasize the relationship between the exit time τ^e and the escape path, we often write $\tau^e(\varphi^a)$ for the exit time of φ^a.

Definition 9.2 *Let $\mathcal{B}^a$ be the set of all escape paths for (9.35) with gain function $a > 0$. An escape path φ with exit time τ^e is a dominant escape path if $\forall \rho > 0$*

$$\lim_{a \to 0} \Pr\left(\sup_{\tau \in [0,\tau^e]} |\varphi(\tau) - \varphi^a(\tau)| < \rho : \mathcal{B}^a\right) = 1. \tag{9.36}$$

Since γ^s is the stable point of the associated o.d.e., the unconditional probability of escaping from the neighborhood of γ^s converges to 0 as $a \to 0$:

$$\lim_{a\to 0} \Pr\left(\mathcal{B}^a\right) = 0.$$

Therefore, in order to define the dominant escape path, we must consider the probability distribution *conditioned on* $\mathcal{B}^a$. In this sense, we are searching for the most likely unlikely events.

9.4 Characterization

Suppose that v_{it} is drawn from a multinomial distribution with mean 0. In order to simplify notation, let us assume that the distribution of v_{it} is symmetric: there exist

$$0 < \sigma_{i1} < \cdots < \sigma_{i\ell} \quad i = 1, 2$$

such that

$$\Pr\left(v_{it} = \sigma_{ik}\right) = \Pr\left(v_{it} = -\sigma_{ik}\right) = p_{ik} \quad k = 1, \ldots, \ell \tag{9.37}$$

and

$$\sum_{k=1}^{\ell} p_{ik} = \frac{1}{2} \quad \forall i \in \{1, 2\}.$$

Let

$$\sigma_i \in \{-\sigma_{i\ell}, \ldots, -\sigma_{i1}, \sigma_{i1}, \ldots, \sigma_{i\ell}\}$$

be a generic element in the support of v_{it}. Let $\sigma = (\sigma_1, \sigma_2)$ be realization of v_t. Since v_{it} $(i = 1, 2)$ takes one of 2ℓ different values, $v_t = (v_{1t}, v_{2t})$ can take one of $4\ell^2$ different values.

Recall that in (8.33), the evolution of $\gamma_{0,t}$ and $\gamma_{1,t}$ is influenced by a common factor $z(\gamma_t, v_t)$. One can easily verify that if γ is in the small neighborhood of γ^s, then

$$z(\gamma, (\sigma_1, \sigma_2))z(\gamma, (-\sigma_1, \sigma_2)) < 0. \tag{9.38}$$

By (8.34), the vector field $\{b(\gamma^s, v_t)\}$ around the stable point γ^s consists of $2\ell^2$ *pairs* of linearly dependent vectors:

$$\exists \rho \in \Re, \quad b(\gamma, (\sigma_1, \sigma_2) = \rho b(\gamma, (-\sigma_1, \sigma_2)). \tag{9.39}$$

By (9.38), this pair of linearly dependent vectors must point in opposite directions:

$$\rho < 0. \tag{9.40}$$

To approach the boundary of $\mathcal{D}$ requires a sequence of "unusual" events of v_t, whose probability is strictly less than 1. Thus, in order to maximize the probability of escape, the escape path must minimize the number of "unusual" events to reach the neighborhood of the exit point. To do so, the adjustment $b(\varphi, v_t)$ made in each period must point in the same direction, say toward the boundary of $\mathcal{D}$. Otherwise, some moves cancel others, wasting precious time to escape. Therefore, at any time τ along the shortest path φ, the vectors in $\{b(\varphi(\tau), v_t)\}$ must point in the same direction: the cone spanned by the vectors must be contained in a closed half space rather than cover $\Re^2$.

To state the first characterization result, we need more notation. Given $b^1, \ldots, b^L \in \Re^2$, let

$$\mathbf{C}(\{b^1, \ldots, b^L\})$$

be the cone spanned by $b^1, \ldots, b^L$. Given $b \in \Re^2$, let

$$\mathbf{H}(b) = \{x : b \cdot x = 0\}$$

be the hyperplane with directional vector b. Let $\mathbf{H}^+(b)$ be the open half space above $\mathbf{H}(b)$. Let $\lceil \tau \rceil$ be the integer part of $\tau \in \Re$. Let

$$f^a_{s,\tau}(\sigma) = \frac{\#\{t : \lceil \tau/a \rceil \leq t \leq \lceil \frac{\tau+s}{a} \rceil, v_t = \sigma\}}{\lceil s/a \rceil} \tag{9.41}$$

be the empirical frequency of σ in time interval $[\tau, \tau + s)$. Define

$$f_{s,\tau}(\sigma) = \lim_{a \to 0} f^a_{s,\tau}(\sigma) \tag{9.42}$$

and

$$f_\tau(\sigma) = \lim_{s \to 0} f_{s,\tau}(\sigma). \tag{9.43}$$

Proposition 9.3 *Suppose that v_{it} $(i = 1, 2)$ has the multinomial distribution described in (9.37). Fix the dominant escape path φ with $\gamma^e \in \partial\mathcal{D}$ with exit time τ^e. Then $\forall \tau \in (0, \tau^e)$, there exist $\overline{s} > 0$ and $b \in \Re^2$ such that $\forall s \in (0, \overline{s})$,*

$$\mathbf{C}(\{b(\varphi(\tau), \sigma) : f_{s,\tau}(\sigma) > 0\}) \subset \mathbf{H}^+(b). \tag{9.44}$$

In particular, if v_{it} $(i = 1, 2)$ has a binomial distribution $(\ell = 1)$, then for $\forall \tau \in (0, \tau^e)$, the support of f_τ is either a singleton or consists of 2 elements, say σ and σ', such that $b(\varphi(\tau), \sigma)$ and $b(\varphi(\tau), \sigma')$ are linearly independent.

Proof. See Appendix A.

The key implication of Proposition 9.3 is that along the dominant escape path, not every σ in the support of v_t can be realized with positive frequency. Hence, the maximum number of elements in the support of f_τ along the dominant path must be strictly less than $4\ell^2$.

In order to find the upper bound for the number of elements in the support of f_τ implied by Proposition 9.3, we need to find a subset $\Sigma(\tau)$ in the support of v_t such that

$$\{b(\gamma, \sigma) : \sigma \in \Sigma(\tau)\}$$

is contained in a half space. Here, we use (9.39) and (9.40) in a crucial way.

Choose an arbitrary $\gamma = \gamma(\tau)$ along the dominant escape path and an arbitrary realization (σ_1, σ_2) of v_t. Consider hyperplane $\mathbf{H}(b) \subset \Re^2$ (or a straight line) that "embeds" $b(\gamma, (\sigma_1, \sigma_2))$:

$$b \cdot b(\gamma, (\sigma_1, \sigma_2)) = 0$$

since b is the norm vector of the hyperplane. We can always choose b so that b and $b(\gamma, (\sigma_1, \sigma_2))$ form 90 degree counter-clockwise.

By (9.39),

$$b \cdot b(\gamma, (-\sigma_1, \sigma_2)) = 0.$$

Starting from $b(\gamma, (\sigma_1, \sigma_2))$, one can select the vectors $b(\gamma, \cdot)$ counter-clockwise until one reaches $b(\gamma, (-\sigma_1, \sigma_2))$, which forms 180 degree with the starting "point" $b(\gamma, (\sigma_1, \sigma_2))$. By (9.40), the number of vectors in $\{b(\gamma, \cdot)\}$ that form less than 180 degree counter-clockwise with $b(\gamma, (\sigma_1, \sigma_2))$ is exactly one half of the total number of vectors in $\{b(\gamma, \sigma)\}$.

Since σ can take as many as $4\ell^2$ different values, there are $4\ell^2$ vectors in $\{b(\gamma, \sigma)\}$. Hence, for each (σ_1, σ_2), one can identify exactly $2\ell^2$ realizations of v_t, each of which induces $b(\gamma, \sigma)$ which forms less than 180 degree counter-clockwise with $b(\gamma, (\sigma_1, \sigma_2))$.

One can repeat the same exercise for each realization of v_t. Thus, there are as many as $4\ell^2$ different collections of perturbations, each of which contains precisely $2\ell^2$ realizations of v_t so that (9.44) holds. Proposition 9.3 implies that the number of elements in the support of f_τ along the dominant escape path cannot exceed $2\ell^2$.

Yet Proposition 9.3 admits that the support of f_τ can have fewer than $2\ell^2$ elements. A standard result of stochastic approximation (e.g., Kushner and Yin (1997)) is that as the gain function $a \to 0$, the sample paths generated by the stochastic algorithm (5.19) converge to the trajectory of the mean dynamics (6.29) in probability. Following the same logic, we prove that the sample paths must converge to the trajectory of the mean dynamics conditioned on (9.44). For example, if v_{it} is drawn from a binomial distribution, the sample paths generated by two linearly independent $b(\gamma, \sigma)$ and $b(\gamma, \sigma')$ must converge to its mean dynamics conditioned on the event $\{v_t = \sigma \text{ or } v_t = \sigma'\}$ with probability 1. In the binomial specification, the probability that $v_t = \sigma$ is $1/4$ for all σ. Therefore, the probability that $v_t = \sigma^i$ $(i = 1, 2)$ conditioned on $v_t \in \{\sigma^1, \sigma^2\}$ is $1/2$.

Proposition 9.4 *Suppose that φ is the dominant escape path with exit time τ^e, and that*

$$g(\sigma) = \Pr(v_t = \sigma).$$

Then for $\forall \tau \in (0, \tau^e)$,

$$\dot{\varphi}(\tau) = \sum_\sigma b(\varphi(\tau), \sigma) g(\sigma : \Sigma(\tau)) \tag{9.45}$$

where $\Sigma(\tau)$ satisfies

$$\mathbf{C}\left(\{b(\varphi(\tau), \sigma) : \sigma \in \Sigma(\tau)\}\right) \subset \mathbf{H}^+(b) \tag{9.46}$$

for some $b \in \Re^s$. In particular, if v_{it} $(i = 1, 2)$ is drawn from a binomial distribution, there exists a pair (σ, σ') such that $b(\varphi(\tau), \sigma)$ and $b(\varphi(\tau), \sigma')$ are linearly independent and

$$\frac{d\varphi(\tau)}{dt} = \frac{1}{2} b(\varphi(\tau), \sigma) + \frac{1}{2} b(\varphi(\tau), \sigma'). \tag{9.47}$$

Proof. See Appendix B.

Since the dominant escape path is one of the trajectories characterized by (9.45), we have to examine at most $4\ell^2$ different trajectories induced by the different collections of perturbations. Since we can obtain a closed form representation for the ordinary differential equation that dictates the dominant escape path when v_{it} has the binomial distribution, we shall first examine the dominant escape path when v_{it} has the binomial distribution.

9.5 Binomial case

9.5.1 Preliminaries

If v_{it} has the binomial distribution for each $i = 1, 2$, then Proposition 9.3 and Proposition 9.4 imply that along the dominant escape path φ with exit time τ^e, there exists a pair (σ, σ') such that $\forall \tau \in (0, \tau^e)$, f_τ is precisely the probability distribution of v_t conditioned on $\{\sigma, \sigma'\}$.

The vector field $\{b(\gamma, v_t)\}$ around $\gamma \in \mathcal{D}$ consists of two pairs of linearly dependent vectors. We can select at most four pairs of linearly independent vectors, and calculate the conditional mean dynamics. If $v_t \in \{(\sigma_1, \sigma_2), (-\sigma_1, -\sigma_2)\}$, then the associated conditional ordinary differential equation is

$$\dot{\varphi} = R^{-1} \begin{bmatrix} U^* - \frac{\varphi_0}{1+\varphi_1^2} \\ -\frac{\varphi_0\varphi_1}{1+\varphi_1^2}\left(U^* - \frac{\varphi_0}{1+\varphi_1^2}\right) - (\theta + \varphi_1)\sigma_2^2 + \sigma_1\sigma_2 \end{bmatrix} \tag{9.48}$$

which has the stable point

$$\gamma^{1,e} = \left(U^*\left[-\theta + \frac{\sigma_1}{\sigma_2}\right]^2, -\theta + \frac{\sigma_1}{\sigma_2}\right),$$

depicted in Figure 9. If $v_t \in \{(\sigma_1, -\sigma_2), (-\sigma_1, \sigma_2)\}$, then the associated conditional ordinary differential equation is

$$\dot{\varphi} = R^{-1} \begin{bmatrix} U^* - \frac{\varphi_0}{1+\varphi_1^2} \\ -\frac{\varphi_0\varphi_1}{1+\varphi_1^2}\left(U^* - \frac{\varphi_0}{1+\varphi_1^2}\right) - (\theta + \varphi_1)\sigma_2^2 - \sigma_1\sigma_2 \end{bmatrix} \tag{9.49}$$

which has the stable point

$$\gamma^{2,e} = R^{-1}\left(-\theta - \frac{\sigma_1}{\sigma_2}, U^*\left(1 + \left[-\theta - \frac{\sigma_1}{\sigma_2}\right]^2\right)\right).$$

If $v_t \in \{(\sigma_1, \sigma_2), (\sigma_1, -\sigma_2)\}$, then the associated conditional ordinary differential equation is

$$\dot{\varphi} = R^{-1} \begin{bmatrix} U^* - \frac{\varphi_0}{1+\varphi_1^2} + \sigma_1 \\ -\frac{\varphi_0\varphi_1}{1+\varphi_1^2}\left(U^* - \frac{\varphi_0}{1+\varphi_1^2} + \sigma_1\right) - (\theta + \varphi_1)\sigma_2^2 \end{bmatrix} \tag{9.50}$$

which has the stable point

$$\gamma^{3,e} = (-\theta, (U^* + \sigma_1)(1 + \theta^2)).$$

If $v_t \in \{(-\sigma_1, \sigma_2), (-\sigma_1, -\sigma_2)\}$, then the associated conditional ordinary differential equation is

$$\dot{\varphi} = R^{-1} \begin{bmatrix} U^* - \frac{\varphi_0}{1+\varphi_1^2} - \sigma_1 \\ -\frac{\varphi_0 \varphi_1}{1+\varphi_1^2} \left(U^* - \frac{\varphi_0}{1+\varphi_1^2} - \sigma_1 \right) - (\theta + \varphi_1)\sigma_2^2 \end{bmatrix} \tag{9.51}$$

which has the stable point

$$\gamma^{4,e} = (-\theta, (U^* - \sigma_1)(1 + \theta^2)).$$

Notice the relationship between $\gamma^{j,e}$ $(j = 1, \ldots, 4)$ and the perturbations that generate each ordinary differential equation. For example, (9.48) is generated by $v_t \in \{(\sigma_1, \sigma_2), (-\sigma_1, -\sigma_2)\}$ which has $\gamma^{1,e}$ as its stable point. As depicted in Figure 9, $\gamma^{1,e}$ is the intersection of

$$\{\gamma : z(\gamma, (\sigma_1, \sigma_2)) = 0\}$$

and

$$\{\gamma : z(\gamma, (-\sigma_1, -\sigma_2)) = 0\}.$$

9.5.2 The dominant escape path

For the binomial case, from an infinity of possible escape paths, we have now narrowed the set of most likely paths down to four, namely, the solutions of the four o.d.e.'s (9.48), (9.49), (9.50), (9.51). We now narrow down the paths more. We can dispose of two of the four candidate escape paths easily, because they fail to escape far enough from the self-confirming equilibrium. The remaining two paths do escape far enough but do so at different rates. The path that escapes *faster* is the dominating escape route. To evaluate which of these two remaining candidate escape paths escapes faster requires analyzing a pair of nonlinear ordinary differential equations. We do this numerically. The trajectory induced by (9.48) is the dominant path, because along this path, γ_t escapes from the neighborhood of γ^s most quickly. Thus, the dominant escape path is the trajectory of (9.48), along which γ_t moves very quickly from γ^s to $\gamma^{1,e}$. We shall verify numerically that this path passes through the γ associated with the Ramsey outcome. This path affirms and explains the simulations.

Before turning to the numerical solutions of the o.d.e.'s, we give some local analytical results.

9.5.3 Details

We can obtain an analytic characterization of the dominant path in a small neighborhood of γ^s. We are interested in the dynamics of recursive algorithm (5.19) when σ_1 and σ_2 are small. Notice that

$$|\gamma^s - \gamma^{3,e}| \to 0$$

and

$$|\gamma^s - \gamma^{4,e}| \to 0$$

as $\sigma^1 \to 0$. Hence, for a recursive algorithm with small perturbations (a "nearly deterministic system"), escaping to $\gamma^{3,e}$ or $\gamma^{4,e}$ makes little difference from staying in the small neighborhood of γ^s, because $\gamma^{3,e}$ and $\gamma^{4,e}$ themselves are in the "small" neighborhood of γ^s.

For this reason, we choose as $\mathcal{D}$ a ball around γ^s with radius large enough to include $\gamma^{3,e}$ and $\gamma^{4,e}$ in the interior, but small enough to exclude $\gamma^{1,e}$ and $\gamma^{2,e}$. Then the only possible candidates for the dominant escape path are

$$\dot{\varphi} = R^{-1} \begin{bmatrix} U^* - \frac{\varphi_0}{1+\varphi_1^2} \\ -\frac{\varphi_0\varphi_1}{1+\varphi_1^2}\left(U^* - \frac{\varphi_0}{1+\varphi_1^2}\right) - (\theta + \varphi_1)\sigma_2^2 + \sigma_1\sigma_2, \end{bmatrix} \tag{9.52}$$

for which $\gamma^{1,e}$ is the stable point, and

$$\dot{\tilde{\varphi}} = R^{-1} \begin{bmatrix} U^* - \frac{\tilde{\varphi}_0}{1+\tilde{\varphi}_1^2} \\ -\frac{\tilde{\varphi}_0\tilde{\varphi}_1}{1+\tilde{\varphi}_1^2}\left(U^* - \frac{\tilde{\varphi}_0}{1+\tilde{\varphi}_1^2}\right) - (\theta + \tilde{\varphi}_1)\sigma_2^2 - \sigma_1\sigma_2 \end{bmatrix} \tag{9.53}$$

for which $\gamma^{2,e}$ is the stable point.

To discriminate between the two remaining trajectories, we need to compare the size of the norm of $\dot{\varphi}$ and $\dot{\tilde{\varphi}}$ around γ^s to see how quickly γ is pushed away from γ^s to $\partial\mathcal{D}$. Since the right hand side of (9.52) is continuously differentiable,

$$\begin{aligned} \dot{\varphi}(\tau) &= \dot{\varphi}(0) + \frac{d\varphi(\tau)}{d\tau}\tau + O(\tau^2) \\ &= \dot{\varphi}(0) + \left[\frac{\partial\varphi(0)}{\partial\varphi_0}\frac{d\varphi_0}{dt} + \frac{\partial\varphi(0)}{\partial\varphi_1}\frac{d\varphi_1}{dt}\right]\tau + \frac{\partial\varphi(0)}{\partial x}\frac{dx}{dt}\tau + O(\tau^2). \end{aligned}$$

A straightforward calculation shows that

$$\left(\dot{\varphi}(0) + \left[\frac{\partial\dot{\varphi}(0)}{\partial\varphi_0}\frac{d\varphi_0}{dt} + \frac{\partial\dot{\varphi}(0)}{\partial\varphi_1}\frac{d\varphi_1}{dt}\right]\tau\right) + \left(\dot{\tilde{\varphi}}(0) + \left[\frac{\partial\dot{\tilde{\varphi}}(0)}{\partial\tilde{\varphi}_0}\frac{d\tilde{\varphi}_0}{dt} + \frac{\partial\dot{\tilde{\varphi}}(0)}{\partial\tilde{\varphi}_1}\frac{d\tilde{\varphi}_1}{dt}\right]\tau\right) = 0 \tag{9.54}$$

and

$$\dot{\varphi}_0(0) + \left[\frac{\partial\dot{\varphi}_0(0)}{\partial\varphi_0}\frac{d\varphi_0}{dt} + \frac{\partial\dot{\varphi}_0(0)}{\partial\varphi_1}\frac{d\varphi_1}{dt}\right]\tau < 0. \tag{9.55}$$

One can show that

$$\left.\frac{\partial\dot{\varphi}(0)}{\partial x}\frac{dx}{dt}\right|_{\varphi} - \left.\frac{\partial\dot{\tilde{\varphi}}(0)}{\partial x}\frac{dx}{dt}\right|_{\tilde{\varphi}} = \begin{bmatrix} -\frac{\gamma_0^s(\gamma_1^s)^2\sigma_1^2}{(1+(\gamma_1^s)^2)} \\ 0 \end{bmatrix}. \tag{9.56}$$

Note that the first element of the vector in (9.56) is negative. Combining (9.54) and (9.55) with (9.56), we conclude that there exists $\overline{\tau} > 0$ such that

$$\|\dot{\varphi}(\tau)\| > \|\dot{\tilde{\varphi}}(\tau)\| \quad \forall\tau \in (0, \overline{\tau}).$$

This inequality proves that it is much easier to escape from $\mathcal{D}$ through φ than $\tilde{\varphi}$.

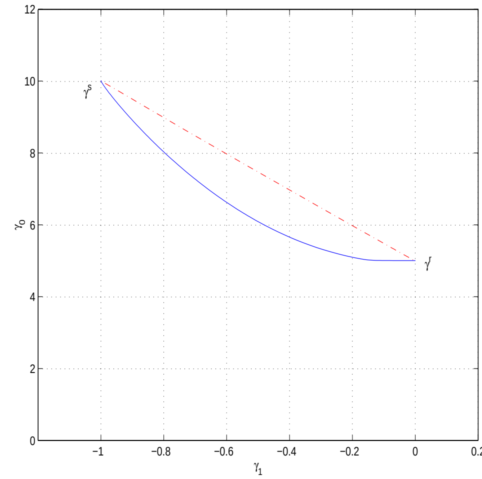

Figure 10: Mean dynamics from γ^r to γ^s (solid line) and shortest escape route dynamics from γ^s to $\partial\mathcal{D}$ (dotted line) with $\sigma_1 = \sigma_2 = .3$.

Proposition 9.5 *There exists $\overline{\Delta} > 0$ such that if the radius of the compact ball $\mathcal{D}$ around γ^s is less than $\overline{\Delta}$, then the dominant escape path is the trajectory of (9.52) with initial condition $\varphi(0) = \gamma^s$.*

Our numerical analysis will further affirm the dominance of trajectory (9.52).

9.5.4 Numerical calculation of dominant escape path

Let γ^r be the belief vector that supports the Ramsey outcome. Figures 10 and 11 display the mean dynamics from γ^r to γ^s and the shortest escape dynamics in the *reverse* direction for two settings of (σ_1, σ_2) with $U^* = 5, \theta = -1$. The escape dynamics were calculated by solving the differential equations (9.47) for our four different candidate selections of the shocks, and then choosing the path that escaped the fastest. We shall soon compare in detail two of these paths. But first it is fruitful to compare figures 10 and 11 with our simulations. The escape path is the same nearly straight path from γ^s to γ^r that we encountered in our simulations.

Figure (12) compares the two candidate escape routes from (9.48) and (9.49) for an example where $\sigma_1 = .3, \sigma_2 = .25$. Notice that the escape occurs much faster for the path associated with (9.48), leading us to proclaim that it is the dominating escape route. Roughly speaking, it is the dominating path because it takes less times – i.e., requires a shorter and hence more likely sequence of unusual shocks – to happen.

That (9.48) yields the dominating escape path reflects the nonlinear dynamics associated with endogenous experimentation that occur along this path. Via the government's pseudo best response function, the government's response to a change in γ is to alter $\hat{x}$ and thereby produce new observations that help to steepen the empirical Phillips curve. Along the escape path determined by (9.48), this endogenous experimentation *reinforces*

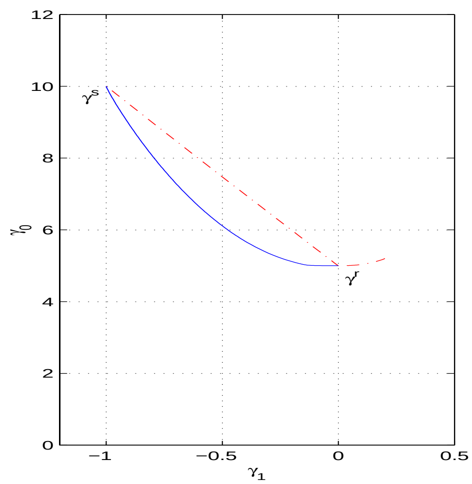

Figure 11: Mean dynamics from γ^r to γ^s (solid line) and shortest escape route dynamics from γ^s to $\partial\mathcal{D}$ (dotted line) with $\sigma_1 = .3, \sigma_2 = .25$.

the effects of the unusual shocks. However, along the escape path determined by (9.49), this endogenous experimentation works against the effects on γ of the unusual shock sequence. (It is a particular shock sequence peculiar to (9.49).) The resistance to the unusual shock sequence caused by the learning from the endogenous experimentation accounts for the slower movement along the escape route determined by (9.49).

Figure 13 shows the solution of the o.d.e. for the dominant escape path for a case in which $\sigma_1 \neq \sigma_2$. In this case, as we have seen, the rest point of the o.d.e. is not the Ramsey value γ^r. But we have already seen from figures 10 and 11 that the path of the o.d.e. passes through the Ramsey value of γ. Figure 13, which shows two snapshots of the same path, with different time scales, shows that the move toward the Ramsey γ is fast, while the subsequent move away from it is very slow. The quickness of the movement toward Ramsey reflects the force in the model whereby endogenous experimentation induces data that appear to come from a vertical Phillips curve. It takes a long time (many more observations) to refine the estimates so that they move to the rest point of the dominant escape path o.d.e. The force toward Ramsey is stronger than the subsequent force toward the fixed point of the escape path o.d.e. This reflects what we remarked upon above, the reinforcement of the move toward Ramsey associated with endogenous experimentation, and the resistance that endogenous experimentation puts to movements away from Ramsey. The *practical* consequence of the slow movement of the escape path dynamics away from Ramsey is to give ample room for the mean dynamics to push γ back toward the Nash equilibrium. This point can be coaxed from figure 14, the bottom panel of which shows the mean dynamics for γ_1 from the Ramsey value toward the self-confirming value γ_1^s. The mean dynamics pushing toward γ^s appear stronger than the escape route dynamics after the Ramsey value for γ_1 has been passed.

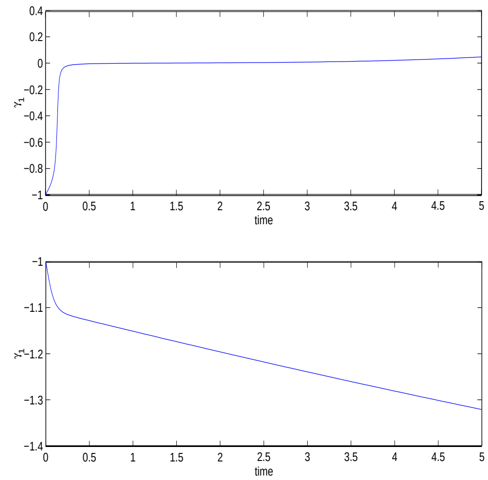

Figure 12: Top panel: the slope γ_1 of the Phillips curve along the shortest (i.e., *fastest* escape route dynamics from γ^s to $\partial\mathcal{D}$ (dotted line) with $\sigma_1 = .3, \sigma_2 = .25$ (from equation (9.48). Bottom panel: the slope γ_1 along the alternative escape path (from equation (9.49)).

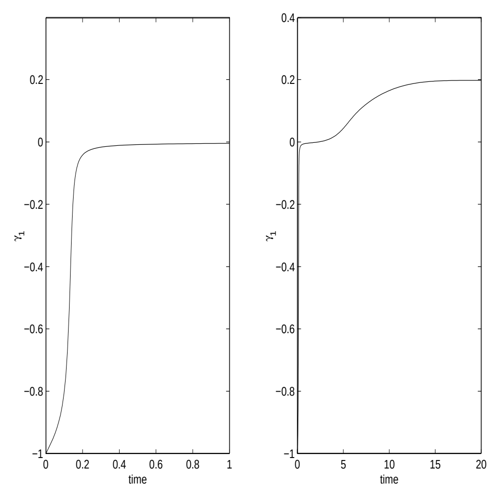

Figure 13: The slope γ_1 of the Phillips curve along the shortest escape route dynamics from γ^s to $\partial\mathcal{D}$ (dotted line) with $\sigma_1 = .3, \sigma_2 = .25$. Note that the escape route passes through the 'natural rate' value $\gamma_1 = 0$ then slowly moves to the rest point of the escape o.d.e. Note the two different time scales.

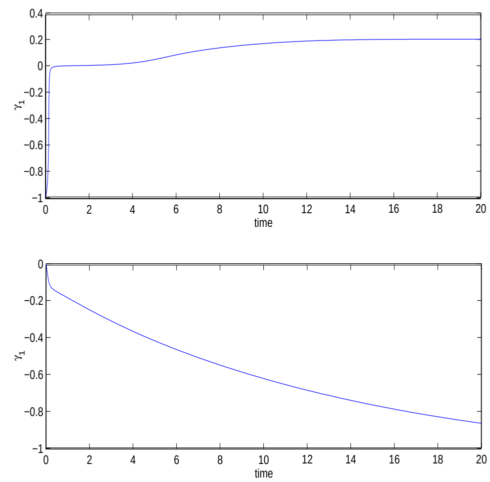

Figure 14: Top panel: the slope γ_1 of the Phillips curve along the shortest (i.e., *fastest* escape route dynamics from γ^s to $\partial\mathcal{D}$ (dotted line) with $\sigma_1 = .3, \sigma_2 = .25$ (from equation (9.48). Bottom panel: the slope γ_1 along the mean dynamics *from* the Ramsey value $\gamma = 0$ toward γ_s.

9.6 Multinomial case

If v_{1t} and v_{2t} have multinomial distributions described in (9.37), then there are as many as $4\ell^2$ different collections of perturbations. Accordingly, we can construct $4\ell^2$ o.d.e.'s conditioned on the collections of perturbations determined by different hyperplanes in (9.44). Let φ_i be the trajectory of (9.45) induced by the i-th collection of perturbations.

Proposition 9.4 implies that the direction of escape is generally determined by the associated hyperplane $\mathbf{H}(b)$. From the remark that follows Proposition 9.3, one can see that we rotate the hyperplane 360 degrees to identify the most likely escape path to every possible direction. Roughly speaking, φ_i is the most likely escape path to the i-th direction. We are trying to identify the most likely "direction" among these $4\ell^2$ candidates.

As we admit much more general distribution, it becomes difficult, if not impossible, to derive a closed form representation of the o.d.e. that dictates the dominant escape path. As a result, we use the numerical method. A good way to visualize the escape dynamics is to solve the $4\ell^2$ o.d.e.'s (9.45) starting from (γ^s, R^s), and then to plot the locus of points $\varphi_i(\tau)$, $i = 1, \ldots, 4\ell^2$ for larger and larger values of τ. For each τ, this locus of points describe the results of a 'race away from Nash' driven by different equally likely possible constellations of unlikely sequences of shocks. The o.d.e. that departs from γ^s fastest is the one whose unusual sequence of shocks is most likely to be observed, conditioning on the rare event of a departure of a given size from γ^s. It is the most likely path because it takes fewer unusual shocks to push a given distance away from γ^s.

We numerically solved the o.d.e.'s for a multinomial distribution with $\ell = 6$ that was chosen to approximate Gaussian distributions for v_{1t}, v_{2t} with standard deviations $(.3, .3)$. We used a simple Euler method for solving the o.d.e.'s. In practice, this meant that we

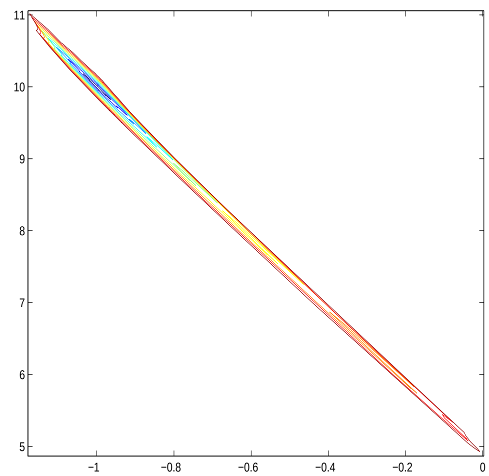

Figure 15: Loci of $\varphi_i(\tau)$ for various values of τ. Larger values of τ have larger loci.

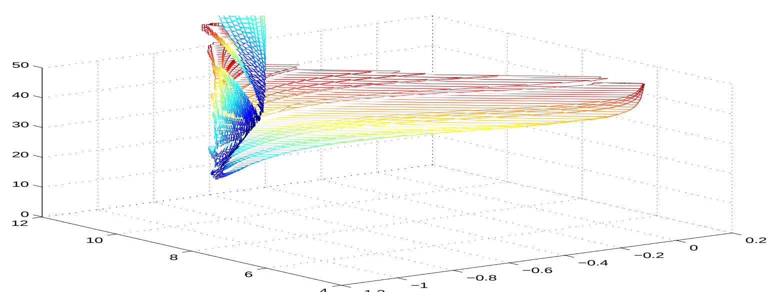

Figure 16: Loci of $\varphi_i(\tau)$ for various values of τ; τ is on the vertical axis.

simply simulated the recursive algorithm itself with fixed a and deterministic shock sequences determined by (9.45). Figure 15 depicts the loci of φ_i for various τ's. Notice how the family of loci are shaped like the escape route from the simulations in figure 6. The dominant escape path points toward Ramsey. Figure 16 shows a three-dimensional view of the loci, where artificial time τ is recorded on the vertical axis.

9.7 General case

If we think of "pricing" unusual shock sequences, we can interpret the most likely escape path as finding the cost-minimizing sequence of v shocks that drives the government's beliefs beyond $\mathcal{D}$. Thus, we no longer require v to be multinomial, only to be such that some functionals below are well defined.[10] Given the recursive formula (5.19), define the H-functional as

$$H(\varphi, \alpha, t) = \lim_{n\to\infty} \frac{1}{n} \log E \exp \left\langle \alpha, \sum_{j=1}^{n} b(\varphi_j, v_j) \right\rangle \tag{9.57}$$

where $\langle\cdot,\cdot\rangle$ is the inner product of two vectors. The action functional is defined to be

$$S(\gamma^s, T, \varphi) = \begin{cases} \int_0^T L(\varphi, \dot{\varphi}, s)ds & \text{if } \varphi \text{ is absolutely continuous} \\ \infty & \text{otherwise} \end{cases} \tag{9.58}$$

with $\varphi(0) = \gamma^s$ where

$$L(x, \beta, t) = \sup_{\alpha} \left[\langle\alpha, \beta\rangle - H(x, \alpha, t)\right]$$

is the LeGendre transformation of the H-functional. The path φ starting at $\varphi = \gamma^s$ and terminating on $\partial\mathcal{D}^o$ that minimizes (9.58) is the dominant escape path. This elegant formulation characterizes how the approximating model behaves as it heads away from a self-confirming equilibrium.

Unfortunately, the characterization suffers because in general neither H nor L has a closed form. Only in very special cases, e.g., Gaussian $b(\varphi, v)$, does H have a convenient form, quadratic in this case.[11] The intractability of H and L for us at this time inspired the alternative approach using the multinomial distribution described above.

Consider a sequence of multinomial distributions for v_t that converge to the normal distribution. At the same time, consider a sequence of the dominant escape paths, each of which is associated with recursive algorithm (9.35) in which v_t has a multinomial distribution. Kushner (1984) points out that the large deviation estimates (such as the dominant escape path) need not converge even if a sequence of distributions converges. At the same time, Kushner (1984) establishes a sufficient condition that if the H functional associated with a multinomial distribution converges, then the large deviation estimates of the limit process of the multinomial distributions also converge.

Note that $b(\varphi, v_t)$ is a smooth function. Thus, as the multinomial distribution converges to the Gaussian distribution weakly, its H functional must converge to the H functional

[10] See Williams (1999) for an analysis based on the approach described in this section.

[11] Even if v_t is distributed normally in our model, $b(\varphi, v)$ is not distributed normally.

when v_t is normally distributed. Thus, the dominant escape path calculated for the multinomial distribution is a reasonable approximation for the dominant escape path when v_t is distributed normally.

Figure 6 reports the escape routes when v_t is distributed normally with $\sigma_1 = \sigma_2 = 0.3$. On the other hand, Figure 15 obtains when v_{it} has a multinomial distribution obtained by discretizing the normal distribution with $\sigma_i = 0.3$ into $2 \times 6 = 12$ grids. The remarkable similarity between the two figures is a consequence of the general result of Kushner (1984).[12]

10 Conclusions

The theme of this paper and Sargent (1999) is how a misspecified non-expectational Phillips curve can approximate an expectational Phillips curve and how the changing quality of that approximation affects government policy and is affected by it. In this paper we have assumed that the government fits a static Phillips curve. This oversimplifies things relative to historical macroeconometric practice, which routinely tried to detect the natural rate hypothesis in terms of the coefficients of a distributed lag Phillips curve. Sargent (1999) studies a generalization of the model in which the government fits a distributed lag Phillips curve. This complicates both the construction of the government's pseudo best response mapping and how the distributed lag Phillips curve can approximate the natural rate hypothesis. Using a distributed lag Phillips curve to approximate the natural rate hypothesis sends us back to issues that arose early in the rational expectations revolution: how econometrically to model anticipated inflation and how to impose invariance of unemployment with respect to anticipated inflation. Before rational expectations, anticipated inflation was modeled as a distributed lag of inflation, often of geometric form, with weights summing to unity. The natural unemployment rate hypothesis was formulated as the restriction that in a regression of inflation on lagged inflation and current and lagged unemployment, weights on lagged inflation should sum to one. Lucas (1972) and Sargent (1971) showed that way of formulating the natural rate hypothesis contradicted rational expectations, except in the special case that inflation has a unit root (see King and Watson (1994)).

Despite Lucas and Sargent, many papers continued to process evidence about the natural rate hypothesis in terms of the sum of weights on inflation in a distributed lag Phillips

[12] Notice that we started with a discrete time recursive algorithm, and then build a continuous time process by taking the linear interpolation of the discrete time process. One may wonder whether we can simplify the analysis by considering the continuous time "limit" of our discrete time process by representing the continuous time process by a diffusion process as in Freidlin and Wentzell (1984). The intuition of the law of large numbers suggests that when the gain function a is sufficiently small, then the continuous time process should be a good approximation of the discrete time process. However, as Kushner (1984) pointed out, the large deviation process of the continuous time "limit" may not be the limit of the large deviation process of the discrete time process, unless the associated H functional converges. While we believe that the large deviation property calculated in this paper should prevail in the continuous time limit, the formal proof remains an open question.

curve.[13] That evidence was against the natural rate hypothesis in the 1960's but came to favor it by the mid 1970's.[14]

Sargent (1999) studies our system in the context of a distribution lag Phillips curve. With the distributed lag Phillips curve, the self-confirming equilibrium again produces the Nash outcome, and the system also recurrently visits an escape route to the Ramsey outcome. Following Chung (1990), Sargent (1999) compared time series of the actual inflation rate y_t with $x_t = h_o(\gamma_t)$, where γ_t now represents the time t estimates of the distributed lag Phillips curve. The estimates indicate that the adaptive algorithms gave timely advice not to exploit the Phillips curve, and lend credibility to the vindication of econometric policy evaluation.

But the vindication is not complete, because the mean dynamics are destined to rekindle inflation unless the government learns a more sophisticated version of the natural rate hypothesis.

[13] See Fuhrer (1995) and King and Watson (1994).

[14] It has recently started pointing against the natural rate again. See Solow and Taylor (1998).

Appendices

A Proof of Proposition 9.3

Let φ be the dominant escape path. If the conclusion of the proposition is false, then we can find $\tau \in (0, \tau^e)$ and $\{s_k\}_{k=1}^{\infty}$ such that

$$s_k \downarrow 0$$

and $\forall s_k > 0$,

$$\mathbf{C}(\{b(\varphi(\tau), \sigma) : f_{s_k,\tau}(\sigma) > 0\}) = \Re^2 \tag{A.59}$$

Lemma A.1 *(A.59) holds, if and only if there exist σ^1, σ^2 and σ^- in the support of $f_{s_k,\tau}$ such that*

$$b(\varphi(\tau), \sigma^-) \in \mathbf{C}\left(\left\{-b(\varphi(\tau), \sigma^1), -b(\varphi(\tau), \sigma^2)\right\}\right). \tag{A.60}$$

If σ^1, σ^2 and σ^- satisfy (A.60), then any permutation of the three vectors satisfy (A.60).

Proof of Lemma A.1. The sufficiency is straightforward, and therefore its proof is omitted. To prove the necessity, assume (A.59).

Note that in order to satisfy (A.59), the support of $f_{s_k,\tau}$ must contain at least three elements. Suppose that the support contains exactly three elements whose cone cover the entire $\Re^2$. Fix an arbitrary pair σ^1 and σ^2 in the support of $f_{s_k,\tau}$. We claim that for the remaining element σ^3 in the support of $f_{s_k,\tau}$, there exists $\rho^1(\sigma^3), \rho^2(\sigma^3) < 0$ such that

$$b(\varphi(\tau), \sigma^3) = \rho^1(\sigma^3) b(\varphi(\tau), \sigma^1) + \rho^2(\sigma^3) b(\varphi(\tau), \sigma^2).$$

If $\rho^1(\sigma^3), \rho^2(\sigma^3) > 0$, then

$$\mathbf{C}\left(\left\{b(\varphi(\tau), \sigma^1), b(\varphi(\tau), \sigma^2), b(\varphi(\tau), \sigma^3)\right\}\right) = \mathbf{C}\left(\left\{b(\varphi(\tau), \sigma^1), b(\varphi(\tau), \sigma^2)\right\}\right)$$

which is a proper subset of $\Re^2$, violating (A.59). If $\rho^1(\sigma^3) < 0$ and $\rho^2(\sigma^3) > 0$, then

$$\begin{aligned}
& \mathbf{C}\left(\left\{b(\varphi(\tau), \sigma^1), b(\varphi(\tau), \sigma^2), b(\varphi(\tau), \sigma^3)\right\}\right) \\
= \; & \mathbf{C}\left(\left\{b(\varphi(\tau), \sigma^1), b(\varphi(\tau), \sigma^2)\right\}\right) \cup \mathbf{C}\left(\left\{-b(\varphi(\tau), \sigma^1), b(\varphi(\tau), \sigma^2)\right\}\right) \\
= \; & \mathbf{H}(b)
\end{aligned}$$

where $b \in \Re^2$ is orthogonal to $b(\varphi(\tau), \sigma^1)$. Hence, (A.59) is not satisfied. The remaining case in which $\rho^1(\sigma^3) > 0$ and $\rho^2(\sigma^3) < 0$ follows from the same logic.

Let us assume that the support of $f_{s_k,\tau}$ now contains at least 4 elements. Choose a pair of σ^1 and σ^2 from the support of $f_{s_k,\tau}$ such that $b(\varphi(\tau), \sigma^1)$ and $b(\varphi(\tau), \sigma^2)$ are linearly independent. If there is σ^- in the support of $f_{s_k,\tau}$ satisfying (A.60), then the proof of Lemma A.1 is done.

Suppose that there is no such σ^- satisfying (A.60). By (A.59), there must exist a pair of σ^3 and σ^4 such that

$$b(\varphi(\tau), \sigma^3) \in \mathbf{C}\left(\left\{b(\varphi(\tau), \sigma^1), -b(\varphi(\tau), \sigma^2)\right\}\right) \tag{A.61}$$

and

$$b(\varphi(\tau), \sigma^4) \in \mathbf{C}\left(\left\{-b(\varphi(\tau), \sigma^1), b(\varphi(\tau), \sigma^2)\right\}\right),$$

or equivalently, $\exists \rho^j(\sigma^k) > 0$ $(j = 1, 2; k = 3, 4)$ such that

$$b(\varphi(\tau), \sigma^3) = \rho^1(\sigma^3) b(\varphi(\tau), \sigma^1) - \rho^2(\sigma^3) b(\varphi(\tau), \sigma^2)$$

and

$$b(\varphi(\tau), \sigma^4) = -\rho^1(\sigma^4) b(\varphi(\tau), \sigma^1) + \rho^2(\sigma^4) b(\varphi(\tau), \sigma^2).$$

A simple calculation shows that

$$b(\varphi(\tau), \sigma^1) = \frac{\rho^2(\sigma^4) b(\varphi(\tau), \sigma^3) + \rho^2(\sigma^3) b(\varphi(\tau), \sigma^4)}{\rho^1(\sigma^3)\rho^2(\sigma^4) - \rho^1(\sigma^4)\rho^2(\sigma^3)}$$

and

$$b(\varphi(\tau), \sigma^2) = \frac{\rho^1(\sigma^4) b(\varphi(\tau), \sigma^3) + \rho^1(\sigma^3) b(\varphi(\tau), \sigma^4)}{\rho^1(\sigma^3)\rho^2(\sigma^4) - \rho^1(\sigma^4)\rho^2(\sigma^3)}.$$

Since we have assumed that (A.60) is not satisfied, the denominator of the above two equations must be positive, which implies that

$$\mathbf{C}\left(\left\{b(\varphi(\tau), \sigma^1), b(\varphi(\tau), \sigma^1)\right\}\right) \subset \mathbf{C}\left(\left\{b(\varphi(\tau), \sigma^3), b(\varphi(\tau), \sigma^4)\right\}\right).$$

In particular, we can choose σ^3 such that

$$\frac{b(\varphi(\tau), \sigma^3)}{|b(\varphi(\tau), \sigma^3)|} \cdot \frac{b(\varphi(\tau), \sigma^2)}{|b(\varphi(\tau), \sigma^2)|} \in [-1, 0)$$

is minimized. Notice that the inner product must be bounded from below because σ^3 must satisfy (A.61). Similarly, choose σ^4 to minimize

$$\frac{b(\varphi(\tau), \sigma^4)}{|b(\varphi(\tau), \sigma^4)|} \cdot \frac{b(\varphi(\tau), \sigma^1)}{|b(\varphi(\tau), \sigma^1)|} \in [-1, 0).$$

Then, $\mathbf{C}\left(\{b(\varphi(\tau), \sigma^3), b(\varphi(\tau), \sigma^4)\}\right)$ is the largest cone containing $\mathbf{C}\left(\{b(\varphi(\tau), \sigma^1), b(\varphi(\tau), \sigma^1)\}\right)$, and is also the largest cone spanned by any element $b(\varphi(\tau), \sigma)$ where σ is in the support of $f_{s_k,\tau}$. Hence, the cone spanned by any pair of $b(\varphi(\tau), \sigma)$ where σ is in the support of $f_{s_k,\tau}$ is contained in a half space. This contradicts to (A.59).

Next, we prove the last part of Lemma A.1. Suppose that σ^1, σ^2 and σ^- satisfy (A.60). Then, there exists $\rho^1(\sigma^-), \rho^2(\sigma^-) > 0$ such that

$$b(\varphi(\tau), \sigma^-) = -\rho^1(\sigma^-) b(\varphi(\tau), \sigma^1) - \rho^2(\sigma^-) b(\varphi(\tau), \sigma^2).$$

One can write

$$b(\varphi(\tau),\sigma^1) = -\frac{1}{\rho^1(\sigma^-)}b(\varphi(\tau),\sigma^-) - \frac{\rho^2(\sigma^-)}{\rho^1(\sigma^-)}b(\varphi(\tau),\sigma^2)$$

which implies that

$$b(\varphi(\tau),\sigma^1) \in \mathbf{C}\left(\left\{-b(\varphi(\tau),\sigma^-), -b(\varphi(\tau),\sigma^2)\right\}\right).$$

Similarly,

$$b(\varphi(\tau),\sigma^2) \in \mathbf{C}\left(\left\{-b(\varphi(\tau),\sigma^-), -b(\varphi(\tau),\sigma^1)\right\}\right),$$

which proves the last part of Lemma A.1. *Q.E.D.*

Fix $s = s_k > 0$. Let

$$\overline{b}_{s,\tau}(\varphi) = \sum_{\sigma} b(\varphi,\sigma) f_{s,\tau}(\sigma)$$

be the mean directional vector at τ. By Lemma A.1, we can choose σ^1, σ^2 and σ^- such that

$$\mathbf{C}\left(\left\{b(\varphi(\tau),\sigma^1), b(\varphi(\tau),\sigma^2), b(\varphi(\tau),\sigma^3)\right\}\right) = \Re^2.$$

Rename each vector so that

$$\overline{b}_{s,\tau}(\varphi) \in \mathbf{C}\left(\left\{b(\varphi(\tau),\sigma^1), b(\varphi(\tau),\sigma^2)\right\}\right) \tag{A.62}$$

and let $\sigma^3 = \sigma^-$ so that there exist $\rho^1(\sigma^-) > 0$ and $\rho^2(\sigma^-) > 0$ such that

$$b(\varphi(\tau),\sigma^-) = -\rho^1(\sigma^-)b(\varphi(\tau),\sigma^1) - \rho^2(\sigma^-)b(\varphi(\tau),\sigma^2).$$

To simplify notation, let us assume that there is only one such σ^- in the support of $f_{s,\tau}$. The general case follows from exactly the same logic, while the notation becomes significantly more complicated.

Note that for $\omega \in [0,1]$,

$$\begin{aligned}
\overline{b}_{s,\tau}(\varphi) &= \sum_{\sigma} b(\varphi(\tau),\sigma) f_{s,\tau}(\sigma) + O(s) \\
&= \sum_{j=1}^{2}\left[\sum_{\sigma\neq\sigma^-}\rho^j(\sigma)f_{s,\tau}(\sigma) + \rho^j(\sigma^-)f_{s,\tau}(\sigma^-)\right] b(\varphi(\tau),\sigma^j) + O(s) \\
&= \sum_{j=1}^{2}\left[\sum_{\sigma\neq\sigma^-}\rho^j(\sigma)f_{s,\tau}(\sigma) + \omega\rho^j(\sigma^-)f_{s,\tau}(\sigma^-)\right] b(\varphi(\tau),\sigma^j) \\
&\quad +(1-\omega)f_{s,\tau}(\sigma^-)b(\varphi(\tau),\sigma^-) + O(s)
\end{aligned}$$

Since

$$\left[\sum_{\sigma\neq\sigma^-}\rho^j(\sigma)f_{s,\tau}(\sigma)\right] + \rho^j(\sigma^-)f_{s,\tau}(\sigma^-) > 0 \quad \forall j = 1,2,$$

there exists $h^j \in (0,1)$ such that

$$h^j \left[\sum_{\sigma \neq \sigma^-} \rho^j(\sigma) f_{s,\tau}(\sigma) \right] + \rho^j(\sigma^-) f_{s,\tau}(\sigma^-) = 0$$

which implies that

$$f_{s,\tau}(\sigma^-) = -\frac{h^j}{\rho^j(\sigma^-)} \sum_{\sigma \neq \sigma^-} \rho^j(\sigma) f_{s,\tau}(\sigma).$$

Without loss of generality, assume that

$$-\frac{1}{\rho^1(\sigma^-)} \sum_{\sigma \neq \sigma^-} \rho^1(\sigma) f_{s,\tau}(\sigma) < -\frac{1}{\rho^2(\sigma^-)} \sum_{\sigma \neq \sigma^-} \rho^2(\sigma) f_{s,\tau}(\sigma),$$

which implies that

$$h^1 > h^2.$$

Hence,

$$h^1 \left[\sum_{\sigma \neq \sigma^-} \rho^2(\sigma) f_{s,\tau}(\sigma) \right] + \rho^2(\sigma^-) f_{s,\tau}(\sigma^-) > 0.$$

We can write the mean dynamics as

$$\begin{aligned}
\overline{b}_{s,\tau}(\varphi) &= \left[\sum_{\sigma \neq \sigma^-} \rho^1(\sigma)(1-\omega h^1) f_{s,\tau}(\sigma) \right] b(\sigma(\tau), \sigma^1) \\
&\quad + \left[\sum_{\sigma \neq \sigma^-} \rho^2(\sigma)(1-\omega h^1) f_{s,\tau}(\sigma) + \rho^2(\sigma^-)\omega(h^1 - h^2) f(\sigma^-) \right] b(\varphi(\tau), \sigma^2) \\
&\quad + (1-\omega) f_{s,\tau}(\sigma^-) b(\varphi(\tau), \sigma^-) + O(s) \\
&= \left[(1-\omega h^1) \sum_{\sigma \neq \sigma^-, \sigma^2} b(\varphi(\tau), \sigma) f_{s,\tau}(\sigma) \right] \\
&\quad + \left[(1-\omega h^1) f_{s,\tau}(\sigma^2) + \rho^2(\sigma^-)\omega(h^1 - h^2) f_{s,\tau}(\sigma^-) \right] b(\varphi(\tau), \sigma^2) \\
&\quad + (1-\omega) f_{s,\tau}(\sigma^-) b(\varphi(\tau), \sigma^-) + O(s).
\end{aligned}$$

Note that

$$\left(\begin{array}{rl} \left[(1-\omega h^1) \sum_{\sigma \neq \sigma^-, \sigma^2} f_{s,\tau}(\sigma) \right] + & [(1-\omega) f_{s,\tau}(\sigma^-)] \\ + & [(1-\omega h^1) f_{s,\tau}(\sigma^2) + \rho^2(\sigma^-)\omega(h^1 - h^2) f_{s,\tau}(\sigma^-)] \end{array} \right) < 1$$

and that each term inside the bracket is strictly positive for a sufficiently small $\omega \in (0,1)$. We can generate the same mean dynamics through

$$\tilde{f}(\sigma) = \begin{cases} (1-h^1) f_{s,\tau}(\sigma) & \text{if } \sigma \neq \sigma^-, \sigma^2 \\ (1-\omega h^1) f_{s,\tau}(\sigma^2) + \rho^2(\sigma^-)\omega(h^1 - h^2) f_{s,\tau}(\sigma^-) & \text{if } \sigma = \sigma^2 \\ (1-\omega) f_{s,\tau}(\sigma^-) & \text{if } \sigma = \sigma^- \end{cases} \tag{A.63}$$

instead of $f_{s,\tau}$. Since $\sum_\sigma \tilde{f}(\sigma) < 1$, $\tilde{f}$ is not an empirical frequency. After normalization, we have

$$\begin{aligned}\varphi(\tau+s)-\varphi(\tau) &= s\sum_\sigma \tilde{f}(\sigma)\left[\sum_\sigma \frac{\tilde{f}(\sigma)}{\sum_\sigma \tilde{f}(\sigma)} b(\varphi(\tau),\sigma)\right] + sO(s) \\ &= s\left[\sum_\sigma \tilde{f}(\sigma) + O(s)\right]\left[\sum_\sigma \frac{\tilde{f}(\sigma)}{\sum_\sigma \tilde{f}(\sigma)} b(\varphi(\tau),\sigma)\right] + sO(s)\end{aligned}$$

For a sufficiently small $s = s_k > 0$,

$$\sum_\sigma \tilde{f}(\sigma) + O(s) < 1$$

which implies that we can construct a path from $\varphi(\tau)$ to $\varphi(\tau+s)$ which takes $s[\sum_\sigma \tilde{f}(\sigma) + O(s)]$ instead of s.

Let $\hat{\varphi}$ be the escape path obtained by the above modification. Note that we have applied the "modification" of the path between $[\tau, \tau+s)$ to each individual sequence of escape paths $\{\varphi^a\}$ converging to φ. If τ^e is the first exit time for φ, then it takes approximately as many as $\lceil \tau^e/a \rceil$ periods to escape from γ^s to $\partial\mathcal{D}$. Thus, the probability of each escape path φ^a is proportional to $(2\ell)^{-\lceil \tau^e/a \rceil}$, since the probability of each realization of v_t is $(2\ell)^{-1}$.

Given an escape path $\tilde{\varphi}$ with exit time τ^e, define

$$N^a_\rho(\tilde{\varphi}) = \left\{\varphi^a(\tau) : \sup_{\tau\in[0,\tau^e]} |\varphi^a(\tau) - \tilde{\varphi}(\tau)| < \rho\right\}.$$

For each $\{\varphi^a\} \in N^a\rho(\varphi)$, we save the escape time as much as

$$\Delta s = s\left[1 - \sum_\sigma \tilde{f}(\sigma) - O(s)\right]$$

which implies that there exists an exponential gain in probability of realization of each escape path as we move from $N^a_\rho(\varphi)$ to $N^a_\rho(\hat{\varphi})$. On the other hand, as we move from $N^a_\rho(\varphi)$ to $N^a_\rho(\hat{\varphi})$, the number of sample paths converging to $\hat{\varphi}$ may decrease. But, this decrease is at the polynomial rate. Hence, for a sufficiently small $\rho > 0$,

$$\frac{\Pr\left(N^a_\rho(\varphi)\right)}{\Pr\left(N^a_\rho(\hat{\varphi})\right)} \propto \left(\frac{1}{2\ell}\right)^{\lceil \Delta s/a \rceil} \to 0$$

as $a \to 0$. We have constructed an alternative escape path, which has a neighborhood with a higher probability of escape than the dominant escape path. This contradiction proves the proposition.

B Proof of Proposition 9.4

Consider

$$\mathcal{E}^a_{s,\tau} = \left\{ \varphi^a_\tau : \begin{array}{rcl} \sum_{\sigma\in\Sigma(\tau)} f^a_{s,\tau}(\sigma) & \geq & 1 - O(s) \\ \varphi^a_\tau(s) & = & \varphi^a_\tau(0) + a\sum_{t=\lceil\tau/a\rceil}^{\lceil\frac{\tau+s}{a}\rceil} b(\varphi^a_t, v_t) \end{array} \right\} \tag{B.64}$$

where $\Sigma(\tau)$ is defined in (9.46), and let $\mathcal{P}^a_{s,\tau}$ be the probability distribution over $\mathcal{E}^a_{s,\tau}(\sigma,\sigma')$. Roughly speaking, $\mathcal{E}^a_{s,\tau}$ is the set of all sample paths where $f_{s,\tau}(\sigma)$ is "almost" concentrated over $\Sigma(\tau)$.

We claim that as $a \to 0$, $\mathcal{P}^a_{s,\tau}$ is concentrated at the path induced by

$$\varphi'(\tau) = \sum_\sigma b(\varphi(\tau),\sigma)g(\sigma : \Sigma(\tau)) + O(s). \tag{B.65}$$

By letting $s \to 0$, we obtain (9.47). By following a standard result of stochastic approximation (e.g., Kushner and Yin (1997)), we know

$$\varphi^a_\tau(s) - \varphi^a_\tau(0) - \int_0^s \bar{b}(\varphi(s'))ds' = \sum_{t=\lceil\tau/a\rceil}^{\lceil\frac{\tau+s}{a}\rceil} a\epsilon_t + R(a)$$

where $\bar{b}(\varphi)$ is the expected value of $b(\varphi^a_t, v_t)$ conditioned on $\mathcal{E}^a_{s,\tau}$ when $a > 0$ is arbitrarily small

$$\epsilon_t = b(\varphi^a_t, v_t) - E_t b(\varphi^a_t, v_t),$$

which is the martingale difference, and $R(a)$ is the interpolation error incurred between the Riemann integral and the discrete sum, which disappears as $a \to 0$. Then $\forall c > 0$,

$$\begin{aligned} & \Pr\left(\left|\varphi^a_\tau(s) - \varphi^a_\tau(0) - \int_0^s \bar{b}(\varphi(s'))ds'\right| \geq c\right) \\ = \; & \Pr\left(\left|\sum_{t=\lceil\tau/a\rceil}^{\lceil\frac{\tau+s}{a}\rceil} a\epsilon_t + R(a)\right| \geq c\right) \\ \leq \; & \Pr\left(\left|\max_{\lceil\tau/a\rceil+1\leq T'\leq\lceil\frac{\tau+s}{a}\rceil} \sum_{t=\lceil\tau/a\rceil}^{T'} a\epsilon_t\right| \geq c - R(a)\right) \\ \leq \; & \sum_{t=\lceil\tau/a\rceil}^{\lceil\frac{\tau+s}{a}\rceil} \frac{a^2 E\epsilon_t^2}{(c-R(a))^2} \to 0 \end{aligned} \tag{B.66}$$

as $a \to 0$. In particular, (B.66) implies that

$$\lim_{a\to 0} \Pr\left(\exists s'' \in (0,s), \quad \left|\varphi^a_\tau(s'') - \varphi^a_\tau(0) - \int_0^{s''} \bar{b}(\varphi(s'))ds'\right| \geq c\right) = 0$$

which means that over the interval $[\tau, \tau+s)$, the sample paths are piled up around the mean dynamics conditioned on $\mathcal{E}^a_{s,\tau}$.

C Facts

Figures 17 and 18 display basic facts about the post WWII U.S. inflation-unemployment correlation. The figures contain scatter plots and regression lines of U.S. quarterly inflation and unemployment rates during selected periods. Inflation is measured by the CPI (all items). Unemployment is measured for white males over 20 years of age. Figure 17 plots the cumulative scatter of points from 1954 I to the last quarter of the indicated year. Thus, successive panels of figure 1 add five years of data. The straight line is for the least squares regression

$$U_t = \hat{\gamma}_0 + \hat{\gamma}_1 y_t,$$

where y_t is inflation and U_t is unemployment. Figure 18 displays scatter plots and regression lines for successive clumps of five years of data for the dates indicated.[15]

Figure 17 shows how adding data gradually steepens the unconditional empirical Phillips curve. By the late 1970's the Phillips curve was vertical. Figure 18 indicates the propensity of the Phillips curve to shift while preserving a negative slope. Thus, with a long enough range of historical experience, the unconditional Phillips curve seems vertical; with brief enough historical perspectives, the Phillips curve retains its negative slope but wanders.

[15]The direction of fit (e.g., y on U versus U on y) matters for our story. See King and Watson (1994) and Sargent (1999).

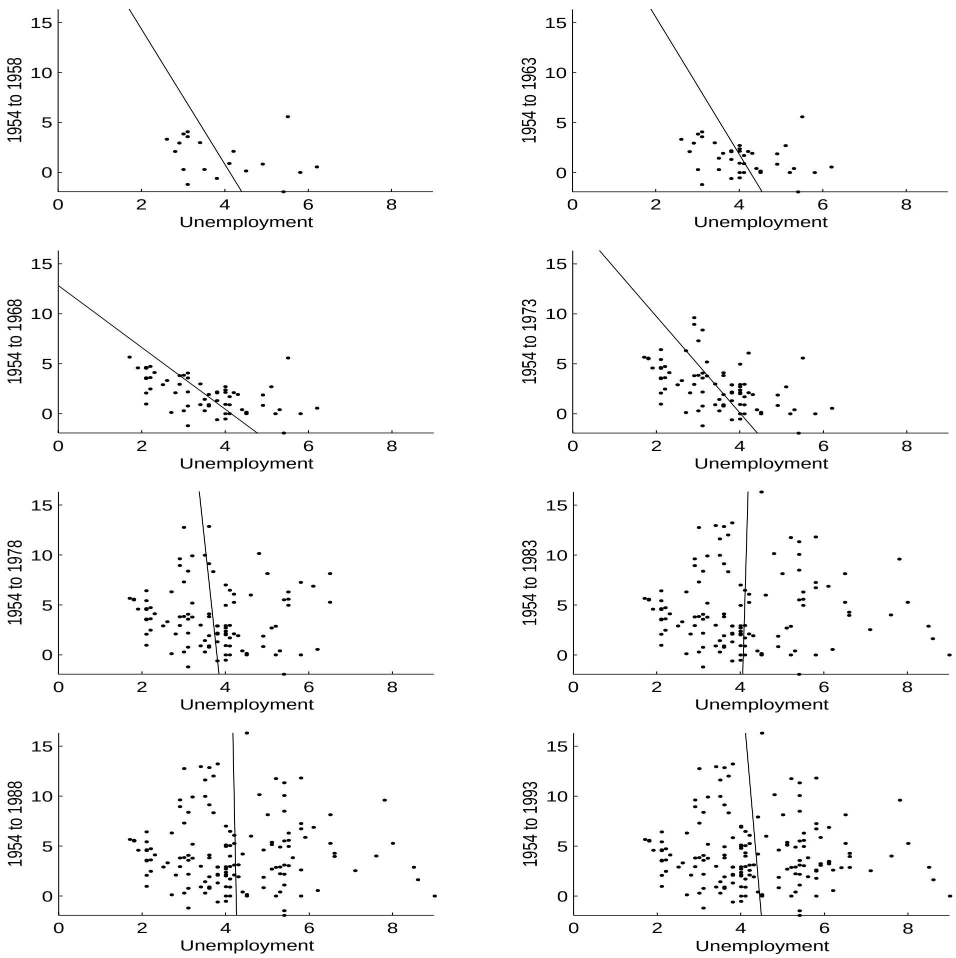

Figure 17: Cumulative scatters of C.P.I. inflation and white male unemployment

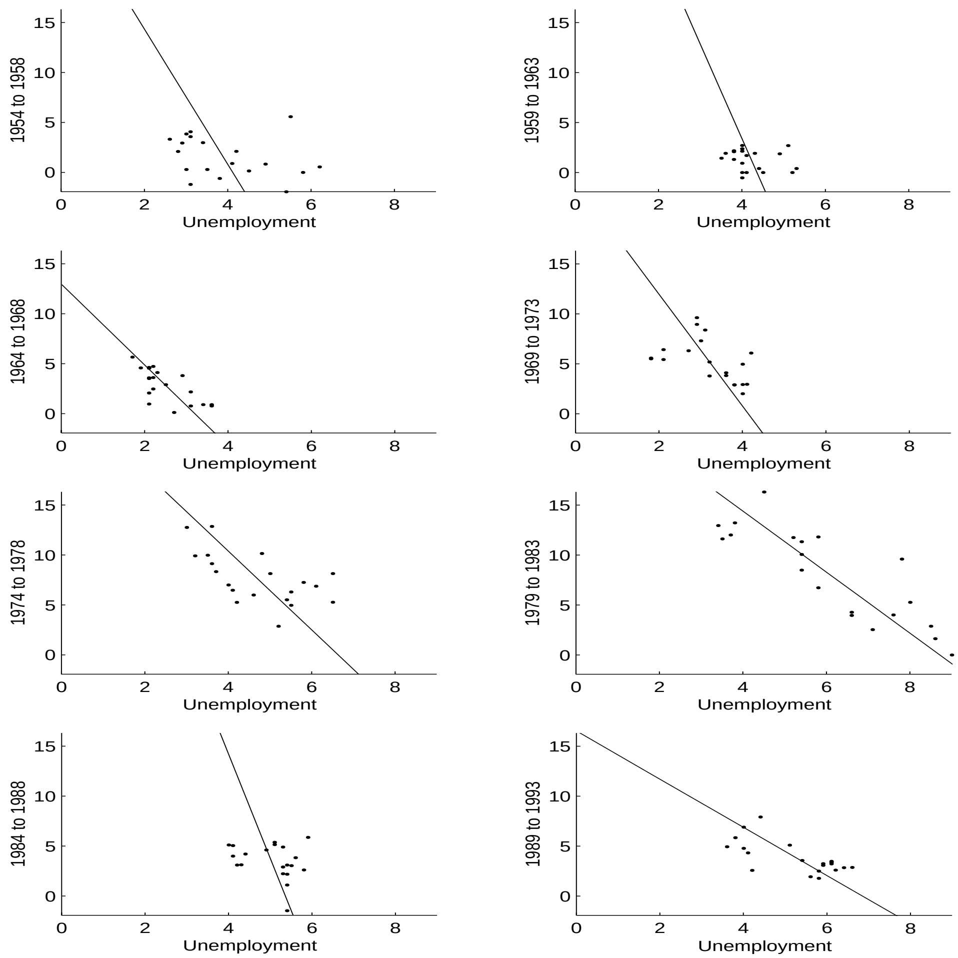

Figure 18: Five year scatters of C.P.I. inflation and white male unemployment

References

Ball, L. (1995). Time consistent policy and persistent changes in inflation. *Journal of Monetary Economics 36*(2), 329–350.

Blinder, A. S. (1998). *Central Banking in Theory and Practice*. M.I.T. Press.

Bray, M. M. (1982). Learning, Estimation and the Stability of Rational Expectations. *Journal of Economic Theory 26*, 318–339.

Bucklew, J. A. (1990). *Large Deviation Techniques in Decisions, Simulation and Estimation*. Wiley.

Cho, I.-K. and A. Matsui (1995). Induction and the Ramsey Policy. *Journal of Economic Dynamics and Control 19*, 1113–1140.

Chung, H. (1990). *Did Policy Makers Really Believe in the Phillips Curve?: An Econometric Test*. Ph. D. thesis, University of Minnesota.

Evans, G. W. and S. Honkapohja (1993). Adaptive Forecasts, Hysteresis and Endogenous Fluctuations. *Economic Review of Federal Reserve Bank of San Francisco 1*, 3–13.

Evans, G. W. and S. Honkapohja (1998). Economic Dynamics with Learning: New Stability Results. *Review of Economic Studies 65*, 23–44.

Evans, G. W. and S. Honkapohja (1999). Learning Dynamics. In J. B. Taylor and M. Woodford (Eds.), *Handbook of Macroeconomics*. Elsevier.

Freidlin, M. I. and A. D. Wentzell (1984). *Random Perturbations of Dynamical Systems*. Springer-Verlag.

Fuhrer, J. C. (1995, March / April). The Phillips Curve is Alive and Well. *New England Economic Review*, 41–55.

Ireland, P. (1997). Does the Time-Consistency Problem Explain the Behavior of Inflation in the United States? *mimeo, Rutgers University*.

Kandori, M., G. Mailath, and R. Rob (1993). Learning, Mutation and Long Run Equilibria in Games. *Econometrica 61*, 27–56.

King, R. G. and M. W. Watson (1994, December). The Post-War U.S. Phillips Curve: A Revisionist Econometric History. *Carnegie-Rochester Conf. Series on Public Policy 41*, 157–219.

Kreps, D. M. (1997). *Anticipated Utility and Dynamic Choice*. Nancy Schwartz Memorial Lecture, Northwestern University.

Kreps, D. M. (1998). *Cooperation, Step-by-Step: How do we learn to trust each other?* David Kinley Lecture at the University of Illinois, Urbana-Champaign.

Kushner, H. J. (1984, February). Robustness and Approximation of Escape Time and Large Deviation Estimates for Systems with Small Noise Effects. *SIAM Journal of Applied Mathematics 44*, 160–182.

Kushner, H. J. and D. S. Clark (1978). *Stochastic Approximation Methods for Constrained and Unconstrained Systems*. Springer-Verlag.

Kushner, H. J. and G. G. Yin (1997). *Stochastic Approximation Algorithms and Applications*. Springer-Verlag.

Kydland, F. and E. C. Prescott (1977). Rules Rather than Discretion: the Inconsistency of Optimal Plans. *Journal of Political Economy 85*, 473–491.

Ljung, L. (1977). Analysis of Recursive Stochastic Algorithms. *IEEE Transactions on Automatic Control*, 551–575.

Lucas, Jr., R. E. (1972). Econometric Testing of the Natural Rate Hypothesis. In O. Eckstein (Ed.), *The Econometrics of Price Determination: Conference, October 1970*. Washington: Board of Governors, Federal Reserve System.

Marcet, A. and J. P. Nicolini (1997). Recurrent Hyperinflations and Learning. *mimeo, Universitat Pompeu Fabra.*

Marcet, A. and T. J. Sargent (1989). Convergence of Least Squares Learning Mechanisms in Self Referential Linear Stochastic Models. *Journal of Economic Theory 48*, 337–368.

McCallum, B. T. (1995). Two Fallacies Concerning Central-Bank Independence. *American Economic Review, Papers and Proceedings 85*, 207–211.

Parkin, M. (1993). Inflation in North America. In K. Shigehara (Ed.), *Price Stabilization in the 1990's*, pp. 47–83.

Sargent, T. J. (1971, August). A Note on the Accelerationist Controversy. *Journal of Money, Credit, and Banking 3*, 721–725.

Sargent, T. J. (1999). *Conquest of American Inflation*. Princeton University Press.

Sims, C. A. (1972). The Role of Approximate Prior Restrictions on Distributed Lag Estimation. *Journal of the American Statistical Association 67*, 169–175.

Sims, C. A. (1988). Projecting Policy Effects with Statistical Models. *Revista de Analisis Economico 3*, 3–20.

Solow, R. M. and J. B. Taylor (1998). *Inflation, Unemployment, and Monetary Policy*. M.I.T. Press.

Stokey, N. L. (1989). Reputation and Time Consistency. *American Economic Review, Papers and Proceedings 79*, 134–139.

White, H. (1982). Maximum Likelihood Estimation of Misspecified Models. *Econometrica 50*, 1–25.

Whittle, P. (1996). *Optimal Control: Basics and Beyond*. Wiley.

Wieland, V. (1997). Learning By Doing and the Value of Optimal Experimentation. *Board of Governors, Federal Reserve System*.

Williams, N. (1999). Analysis of the Convergence and Escape of a Constant Gain Learning Algorithm. *mimeo.*

Woodford, M. D. (1990). Learning to Believe in Sunspots. *Econometrica 58*, 277–307.

Young, P. (1993). The Evolution of Conventions. *Econometrica 61*, 57–83.

European Central Bank Working Paper Series

1 “A global hazard index for the world foreign exchange markets” by V. Brousseau and F. Scacciavillani, May 1999.

2 “What does the single monetary policy do? A SVAR benchmark for the European Central Bank” by C. Monticelli and O. Tristani, May 1999.

3 “Fiscal policy effectiveness and neutrality results in a non-Ricardian world” by C. Detken, May 1999.

4 “From the ERM to the euro: new evidence on economic and policy convergence among EU countries” by I. Angeloni and L. Dedola, May 1999.

5 “Core inflation: a review of some conceptual issues” by M. Wynne, May 1999.

6 “The demand for M3 in the euro area” by G. Coenen and J.-L. Vega, September 1999.

7 “A cross-country comparison of market structures in European banking” by O. de Bandt and E. P. Davis, September 1999.

8 “Inflation zone targeting” by A. Orphanides and V. Wieland, October 1999.

9 “Asymptotic confidence bands for the estimated autocovariance and autocorrelation functions of vector autoregressive models” by G. Coenen, January 2000.

10 “On the effectiveness of sterilized foreign exchange intervention” by R. Fatum, February 2000.

11 “Is the yield curve a useful information variable for the Eurosystem?” by J. M. Berk and P. van Bergeijk, February 2000.

12 “Indicator variables for optimal policy” by L. E. O. Svensson and M. Woodford, February 2000.

13 “Monetary policy with uncertain parameters” by U. Söderström, February 2000.

14 “Assessing nominal income rules for monetary policy with model and data uncertainty” by G. D. Rudebusch, February 2000.

15 “The quest for prosperity without inflation” by Athanasios Orphanides, March 2000.

16 “Estimating the implied distribution of the future short term interest rate using the Longstaff-Schwartz model” by Peter Hördahl, March 2000.

17 “Alternative measures of the NAIRU in the euro area: estimates and assessment” by Silvia Fabiani and Ricardo Mestre, March 2000.

18 “House prices and the macroeconomy in Europe: Results from a structural VAR analysis” by Matteo Iacoviello, April 2000.

19 “The Euro and international capital markets” by Carsten Detken and Philipp Hartmann, April 2000.

20 “Convergence of fiscal policies in the euro area” by O. de Bandt and F. P. Mongelli, May 2000.

21 “Firm size and monetary policy transmission: evidence from German business survey data” by M. Ehrmann, May 2000.

22 “Regulating access to international large value payment systems” by C. Holthausen and T. Rønde, June 2000.

23 “Escaping Nash inflation” by I-K. Cho and T. J. Sargent, June 2000.